

Rapid thinning of the Laurentide Ice Sheet in coastal Maine, USA during late Heinrich Stadial 1

Author: Alexandria Jo Koester

Persistent link: <http://hdl.handle.net/2345/bc-ir:107308>

This work is posted on [eScholarship@BC](#),
Boston College University Libraries.

Boston College Electronic Thesis or Dissertation, 2017

Copyright is held by the author, with all rights reserved, unless otherwise noted.

**Rapid thinning of the Laurentide Ice Sheet in coastal Maine,
USA during late Heinrich Stadial 1**

Alexandria J. Koester

A thesis

Submitted to the Faculty of

the department of Earth and Environmental Science

in partial fulfillment

of the requirements for the degree of

Masters of Science

Boston College
Morrissey College of Arts and Sciences
Graduate School

March 2017

Rapid thinning of the Laurentide Ice Sheet in coastal Maine, USA, during late

Heinrich Stadial 1

Alexandria J. Koester

Advisor: Jeremy D. Shakun, Ph.D.

Abstract

Few data are available to infer the thinning rate of the Laurentide Ice Sheet (LIS) through the last deglaciation, despite its importance for constraining past ice sheet response to climate warming. We measured 31 cosmogenic ^{10}Be exposure ages in samples collected on coastal mountainsides in Acadia National Park and from the slightly inland Pineo Ridge moraine complex, a ~100-km-long glaciomarine delta, to constrain the timing and rate of LIS thinning and subsequent retreat in coastal Maine. Samples collected along vertical transects in Acadia National Park have indistinguishable exposure ages over a 300 m range of elevation, suggesting that rapid, century-scale thinning occurred at 15.2 ± 0.7 ka, similar to the timing of abrupt thinning inferred from cosmogenic exposure ages at Mt. Katahdin in central Maine (Davis et al., 2015). This rapid ice sheet surface lowering, which likely occurred during the latter part of the cold Heinrich Stadial 1 event (19-14.6 ka), may have been due to enhanced ice-shelf melt and calving in the Gulf of Maine, perhaps related to regional oceanic warming associated with a weakened Atlantic Meridional Overturning Circulation at this time. The ice margin subsequently stabilized at the Pineo Ridge moraine complex until 14.5 ± 0.7 ka, near the onset of Bølling Interstadial warming. Our ^{10}Be ages are substantially younger than marine radiocarbon constraints on LIS retreat in the coastal lowlands, suggesting that the deglacial marine reservoir effect in this area was ~1,200 ^{14}C years, perhaps also related to the sluggish Atlantic Meridional Overturning Circulation during Heinrich Stadial 1.

Table of Contents

Table of Contents	iv
List of Tables.....	v
List of Figures	vi
Introduction	1
Background	3
Study Sites.....	9
Methods.....	11
Results	14
Discussion	15
Conclusions	22
Acknowledgments	22
References	23
Figures.....	33
Tables	43
Supplementary Material	45
Supplementary References	56

List of Tables

Table 1: ^{10}Be ages from Acadia National Park and the Pineo Ridge moraine complex

Table S1: Published radiocarbon data

Table S2: Acadia National Park and Pineo Ridge moraine complex ^{10}Be data

List of Figures

Figure 1: Deglaciation in Maine

Figure 2: Sample examples

Figure 3: Map of Acadia National Park

Figure 4: Map of the Pineo Ridge moraine complex

Figure 5: Exposure ages in Acadia National Park

Figure 6: Probability distribution functions (camel plots) of ^{10}Be ages

Figure 7: Monte Carlo Analysis

Figure 8: Paleoclimate records from the Northern Hemisphere compared to Acadia ^{10}Be dipstick ages

Introduction

The largest uncertainty surrounding future sea-level rise concerns dynamic thinning of the polar ice sheets (Pfeffer et al., 2008), which at present may be driven most strongly by ocean warming at their marine margins (Pritchard et al., 2009, 2012; Straneo and Heimbach, 2013). A variety of processes can determine behavior along marine margins, such as unstable retreat of the grounding line on reverse-sloping beds (marine ice sheet instability; Joughin and Alley, 2011), hydrofracturing of ice shelves and unstable ice cliff collapse (marine ice cliff instability; Scambos et al., 2004; Bassis and Walker, 2012), ocean thermal forcing of basal ice-shelf melt (Straneo and Heimbach, 2013), relative sea-level shifts due to changes in ice volume and gravity fields influencing grounding-line position (Gomez et al., 2015), and grounding-zone sedimentation stabilizing ice margins (Alley et al., 2007).

The short instrumental record and the relatively modest changes over this interval are insufficient to assess how these and other factors will affect future ice sheet collapse as climate warming continues. Ice sheet models are rapidly evolving as better representations of the underlying physical processes are incorporated (Schoof, 2007; Gomez et al., 2015; DeConto and Pollard, 2016); these models need data sets against which to test their reliability (DeConto and Pollard, 2016). Pleistocene deglaciations can provide useful case studies to better understand the dynamics of a decaying marine-terminating ice sheet and its interaction with the ocean and atmosphere but only if the timing and rate of past ice sheet collapse in coastal settings can be well dated. The deglaciation of the Laurentide Ice Sheet (LIS) in coastal Maine serves as one such example.

The timing of LIS lateral retreat in terrestrial New England has been constrained using many radiocarbon ages (e.g., Thompson et al., 1999; Dorion et al., 2001; Dyke, 2004), cosmogenic nuclide exposure dating in a few locations (Balco et al., 2002, 2009; Balco and Schaefer, 2006; Bierman et al., 2015; Bromley et al., 2015; Davis et al., 2015), and the New England Varve Chronology in several major river valleys (Ridge et al., 2012). The deglacial chronology remains less certain elsewhere in New England, including coastal Maine (Fig. 1), which was below sea level due to isostatic depression until emergence began at ~ 14 ka (Retelle and Weddle, 2001; Kelley et al., 2010). Deglacial radiocarbon ages from materials, such as shells, are subject to uncertainties in marine reservoir corrections (Kaplan, 1999; Dorion et al., 2001; Retelle and Weddle, 2001; Borns et al., 2004; Thompson et al., 2011; Thompson, 2015). Lake and bog basal radiocarbon ages from above the marine limit typically provide minimum-limiting ages, and may not faithfully constrain deglaciation timing due to lags in vegetation colonization and deposition of organic material (Stuiver and Borns, 1975; Davis and Davis, 1980). Moreover, these data provide little information on the timing and rate of ice sheet thinning, which, for former ice sheets, is notoriously difficult to quantify.

Cosmogenic exposure ages can provide a more direct constraint on ice sheet thickness history than minimum-limiting radiocarbon ages. The timing and rate of thinning can be determined by obtaining a series of cosmogenic exposure ages along vertical transects down mountainsides that melted out of the thinning ice sheet, an approach informally known as glacial ‘dipstick’ dating (Stone et al., 2003). The glacial dipstick method has been used successfully in Antarctica (Stone et al., 2003; Johnson et al., 2014), Europe (Goehring et al., 2008), Greenland (Corbett et al., 2011; Winsor et al.,

2015) and Patagonia (Boex et al., 2013), but has yet to be applied in North America with high-resolution sampling.

Here, we present 18 cosmogenic ^{10}Be surface exposure ages of boulder and bedrock pairs down mountainsides in Acadia National Park and six ^{10}Be exposure ages from the Jordan Pond moraine in the park in order to provide direct information about the timing of vertical ice-sheet thinning in coastal Maine. In addition, we also report seven ^{10}Be exposure ages of boulders from the Pineo Ridge moraine complex (PRMC), a large moraine/glaciomarine delta, to date the timing of ice-sheet margin retreat from coastal Maine (Fig. 1). These data indicate that the LIS thinned rapidly in this area during late Heinrich Stadial 1, and that the ice persisted for several more centuries near the coast before abandoning the PRMC approximately coincident with Bølling warming. The ^{10}Be ages are younger than calibrated radiocarbon-based estimates of deglaciation, suggesting that the deglacial marine reservoir effect in the waters off New England was $\sim 1,200$ ^{14}C years; this value may help refine marine radiocarbon chronologies elsewhere in the region and inform interpretations of paleoceanographic dynamics.

Background

Exposure Dating: Applications and Assumptions

In situ produced ^{10}Be is formed primarily by cosmic ray spallation of oxygen in rock and soil by neutrons, which mostly attenuate within a meter or two below the surface (Gosse and Phillips, 2001). The buildup of ^{10}Be in rock surfaces can thus be inverted to measure how long ago ice retreated and exposed a landscape. Some geological complications can reduce the accuracy of this geochronometer and lead to either overestimates or underestimates of the true age of deglaciation. For instance,

nuclides produced during previous episodes of exposure can be inherited if there was insufficient glacial erosion to remove many meters of material, biasing deglaciation ages so that they are too old (Gosse and Phillips, 2001; Briner et al., 2016). Bedrock may be more likely to contain inherited nuclides than boulders, since the latter have been transported and abraded (Bierman et al., 1999); the collection and age coincidence of boulder-bedrock pairs is thus a means for testing the veracity of exposure ages (Marsella et al., 2000; Briner et al., 2003; Corbett et al., 2013). On the other hand, post-glacial cover by soil and snow cover can shield the underlying surface from cosmic rays, which lowers the production rate of ^{10}Be , causing the apparent age of the sample to underestimate the timing of deglaciation (Schildgen et al., 2005). Likewise, post-glacial subaerial erosion will lead to a younger apparent age because surface material, rich in nuclides, is preferentially lost (Heyman et al., 2011).

Paleoclimate context and New England deglaciation

The last Northern Hemisphere deglaciation was punctuated by several abrupt warming and cooling events well expressed in the Greenland ice core record (Andersen et al., 2004). These climate events were related to variations in the strength of northward heat transport by the Atlantic Meridional Overturning Circulation (AMOC), thought to be linked to meltwater events from ice sheets (Clark et al., 2001; Thornalley et al., 2010). For instance, freshwater forcing related to initial retreat of the Northern Hemisphere ice sheets may have weakened the AMOC beginning ~19 ka, triggering Heinrich Stadial 1 (HS1; 19-14.6 ka), a cooling event in the North Atlantic (McManus et al., 2004; Clark et al., 2009). Following the recovery of the AMOC at 14.6 ka, the Northern Hemisphere experienced abrupt warming into the Bølling-Allerød interstadial. The deglaciation of the

LIS is inherently linked to these perturbations of the overall warming climate (Balco et al., 2002; Kaplan, 2007; Ullman et al., 2014), though the detailed dynamics of the connections remain uncertain.

Over the last several decades, glacial geologic mapping and cosmogenic exposure dating has revealed the maximum extent and pattern of subsequent retreat of the LIS in New England. At the LGM, the southeastern margin of the LIS extended into the Gulf of Maine ~600 km beyond the present coastline and onto Georges Bank (Pratt and Schlee, 1969; Schnitker et al., 2001). Cosmogenic exposure dating indicates that the LIS margin initially pulled back from its maximum extent in southeastern Massachusetts at Martha's Vineyard, dated to 27.5 ± 1.6 ka ($n = 8$), and northern New Jersey, dated to 25.2 ± 1.3 ka ($n = 16$; Corbett et al., 2017; these ages and all those reported below are recalculated using the northeastern North American production rate from Balco et al. (2009) and give uncertainties as the standard error of boulder ages and the production rate uncertainty (4.8%), added in quadrature). Several recessional moraines in southernmost New England also have been dated with ^{10}Be , including the Buzzard's Bay moraine in Massachusetts (20.3 ± 1.0 ka, $n = 10$; Balco et al. (2002)), and the Old Saybrook (20.7 ± 1.1 ka, $n = 7$; Balco and Schaefer (2006)) and Ledyard (20.7 ± 1.0 ka, $n = 7$; Balco and Schaefer (2006)) moraines in southern Connecticut. These ages indicate that retreat was slow and spatially limited until after ~20 ka when Northern Hemisphere summer insolation increased (Clark et al., 2009). It took about 7,000 years for the ice margin to retreat to northern New England and deposit the Littleton-Bethlehem moraine (13.8 ± 0.7 ka, $n = 4$; Balco et al. (2009); Thompson et al. (2017)) in central-northern New

Hampshire, and the Androscoggin moraine (13.2 ± 0.7 ka, $n = 7$; Bromley et al., 2015) in northeastern New Hampshire and western Maine.

The New England varve record also has provided significant insight into the retreat of the LIS in central New England, based on the progressive deposition of glacial varves in proglacial ice-dammed lakes up the length of the Connecticut valley (Ridge et al., 2004, 2012). The record indicates that retreat began slowly (~ 50 m/year) in southern New England, but steadily increased to 300 m/year between 14.7 and 14.1 ka during the Bølling in northern New England (Ridge, 2004, 2012). The ice margin receded from the Connecticut valley into Canada by 13.5 ka (Ridge et al., 2012).

Marine Reservoir Correction in coastal Maine

Because there is a difference between the $^{14}\text{C}/^{12}\text{C}$ ratio of the ocean and that of the contemporaneous atmosphere, a marine reservoir correction is needed to make radiocarbon ages of marine samples comparable to those of terrestrial samples (Waelbroeck et al., 2001). The marine reservoir effect (the offset between the $^{14}\text{C}/^{12}\text{C}$ ratio in the ocean and atmosphere) varies over time and space as a result of changes in ocean circulation (Mangerud, 1972), ^{14}C production rates in the atmosphere (Stuiver et al., 1986), and ventilation between the atmosphere and ocean (Bard et al., 1994). Modern marine reservoir ages are 400 ± 100 years in the North Atlantic (Bard, 1988).

A reservoir correction must be applied to many of the radiocarbon ages in coastal Maine because the material dated is of marine origin, i.e. it lived in the ocean and was deposited in marine sediment when the region was isostatically depressed. The ocean inundated the coast and transgressed up to 175 km inland and ~ 70 m above sea level based on the elevation of topset-forset delta contacts (Thompson et al., 1989). Numerous estimates for the deglacial marine reservoir effect in coastal Maine have been made,

including >400 years (Dorion et al., 2001), 600 years (Borns et al., 2004), >1,000 years (Thompson et al., 2011), and 2,000 years (Ridge et al., 2001).

Deglacial History in Maine

The deglacial history of the LIS in Maine has primarily been constrained with minimum-limiting radiocarbon ages from both terrestrial and marine settings. However, in a few locations, radiocarbon ages come from glaciomarine sediments that are interbedded with ice-proximal and ice-distal facies (e.g. Dennison Point, Pond Ridge moraine), and thus closely limit deglaciation (Kaplan, 1999; Dorion et al., 2001). As discussed above, marine organic material dated by radiocarbon must be corrected for the marine reservoir effect, though other ages in this region are from terrestrial materials deposited on bog and pond bottoms (Borns et al., 2004) for which no marine reservoir correction is needed. However, radiocarbon ages measured on bulk sediment also should be treated cautiously, because the samples may contain some proportion of carbon-bearing material predating the time of deposition (Grimm et al., 2009).

The sedimentary record also reveals how the ice sheet margin evolved during deglaciation. Seismic reflection profiles combined with marine stratigraphy from the Gulf of Maine (Belknap and Shipp, 1991; Schnitker et al., 2001) indicate that a grounded ice sheet transitioned to a marine calving embayment (Borns and Hughes, 1977; Borns, 1985; Hughes et al., 1985) between 20 and 17 ka (Schnitker et al., 2001). The ice margin is estimated to have reached the present coastline between 17 and 16 ka during HS1 (using a 600 year radiocarbon reservoir correction; see Discussion) (Smith, 1985; Kaplan, 1999; Retelle and Weddle, 2001; Borns et al., 2004; Fig. 1), becoming buttressed on underlying bedrock ledges and sills in shallow marine water resembling a modern

tidewater glacier (Tucholke and Hollister, 1973; Crossen, 1991; Kaplan, 1999). Analysis of benthic foraminiferal $\delta^{18}\text{O}$ and faunal assemblages from southeastern coastal Maine indicate that water temperatures were arctic to subarctic during the deglaciation (0-2°C; Dorion et al., 2001). Various deglacial landforms were deposited into shallow water (less than 80 m) along the coast, such as stratified moraines, esker-fed ice-contact deltas, and outwash deltas (Ashely et al., 1999; Borns et al., 2004), collectively forming a coastal moraine belt. Ice deformation features such as folds and faults in stratified deposits indicate that ice was actively flowing during retreat (Koteff and Pessl, 1981; Crossen, 1991; Dorion et al., 2001).

Within the coastal moraine belt, there are two particularly prominent ice-contact Gilbert-style deltas, the PRMC and the Pond Ridge moraine (LePage, 1982). Radiocarbon dating of *in situ* shells within the Pond Ridge moraine bracket its age to between 16.7 and 16.5 cal ka (13.8-13.6 ^{14}C ka; Kaplan, 1999, no reservoir correction), whereas radiocarbon ages from mollusk shells north and south of the PRMC constrain its emplacement age between ~16 and 15 cal ka (13.8-13.4 ^{14}C ka; Kaplan (2007); author assumed a reservoir correction of 400 ^{14}C years on the older age and 600 ^{14}C years on the younger age), during the latter part of HS1. Davis et al. (2015) reported a ^{10}Be age of 16.4 ± 1.1 , a ^{26}Al age of 19.8 ± 1.8 and an uncertainty-weighted average ^{10}Be - ^{26}Al age of 17.5 ± 1.1 ka for one boulder from the PRMC (PTK-17), older than the radiocarbon constraints but still during the cold HS1. Crosscutting relationships within the moraine belt in eastern Maine indicate that the PRMC and likely the Pond Ridge moraine represent a readvance and/or reorganization of the ice margin, though the western portion may represent a stillstand (Kaplan, 1999).

Following deposition of the coastal moraine belt, the ice margin retreated abruptly after the Bølling warming, corresponding with a geomorphic transition from moraines to esker systems (Dorion et al., 2001; Borns et al., 2004). Once the ice sheet retreated further inland, relative sea level rapidly fell after ~14.3 cal ka (~12.2 ¹⁴C ka; Retelle and Weddle, 2001, authors used 600 ¹⁴C year reservoir correction) due to glacial isostatic adjustment, reaching a relative sea-level low stand of -60 m at ~12.5 cal ka (Barnhardt et al., 1997). Relative sea level rose rapidly after ~12.5 cal ka to -20 m below present level, then remained nearly static between ~11.5 and 7.5 cal ka, before approaching modern levels in the mid-Holocene (Kelley et al., 2010).

Although the deglacial chronology in Maine is highly dependent on radiocarbon ages, recent cosmogenic nuclide exposure dating in central Maine also offers insight into ice dynamics during the last deglaciation. Some samples collected on the summits of Katahdin, Maine (Fig. 1), as well as Mount Washington, New Hampshire, contain high concentrations of cosmogenic nuclides inherited from prior periods of exposure (Bierman et al., 2015). Such inheritance likely indicates that thin, cold-based ice covered these peaks, causing little erosion. Nonetheless, other samples on the Katahdin edifice (~1300-1600 m asl) appear to have been deeply eroded before exposure at deglaciation as they yield an average age of 15.3 ± 1.1 ka ($n = 6$), indistinguishable from boulders on the Basin Ponds moraine, part way down the mountain (~750 m asl; 16.1 ± 0.9 ka; $n = 5$), as well as Pockwockamus Rock in the nearby lowlands (150 m asl; 14.5 ± 0.8 ka). Together, these data suggest rapid drawdown of the ice sheet between 16 and 15 ka in central Maine (Davis et al., 2015).

Study Sites

We used ^{10}Be to date deglaciation in three areas of coastal Maine: vertical transects in Acadia National Park, the Jordan Pond moraine in Acadia National Park, and the PRMC, about 50 km northeast of Acadia National Park. All sample locations in Acadia National Park were above the marine limit (70 m asl).

Acadia National Park is located on Mount Desert Island, along the south-central coast of Maine (Fig. 1). Several peaks rise above 350 m asl, including Cadillac Mountain (466 m asl), the highest coastal point in the eastern United States. Most of Acadia National Park is underlain by the Devonian pink coarse-grained Cadillac Mountain Granite (Gilman et al., 1988). Two basal radiocarbon ages have been reported from Sargent Mountain Pond (336 m asl; above the marine limit) on Mount Desert Island, providing a minimum constraint on when the area emerged from beneath the ice sheet. Lowell (1980) dated bulk sediments 1.33 m above the base of a core to 15.7 ± 0.7 cal ka (13.25 ± 0.26 ^{14}C ka), while Norton et al. (2011) more recently obtained a similar basal age of 15.7 ± 0.4 cal ka (13.26 ± 0.05 ^{14}C ka) on unspecified organic sediment 7 cm above refusal from a different core.

Jordan Pond is located in central Acadia National Park between Penobscot Mountain and Pemetic Mountain at an elevation of 83 m asl. Once the ice sheet reached coastal Maine and thinned sufficiently to expose peaks, ice lobes formed in the major valleys (Gilman et al., 1988). One such lobe deposited an end moraine just above the marine limit that serves as a natural dam at the southern end of Jordan Pond (Graham, 2010). The Jordan Pond moraine is thus the most proximal moraine to the coast that was not affected by marine inundation.

The PRMC is ~100 km long and located ~20 km from the current coastline in southeastern Maine at an elevation of ~70 m asl, just below the marine limit (Fig. 1; Borns et al., 2004). Parts may have initially been under water, but any submergence was likely brief due to rapid postglacial rebound (Borns et al., 2004; Kelley et al., 2010). Morphologically, the PRMC is a sharp-crested morainal bank that spatially transitions to a flat-topped morainal bank (Hunter and Smith, 2001); it was formed at the grounding line in marine conditions, as demonstrated by the presence of marine silt and clay, a change in sediment facies between the ice-proximal and ice-distal side of the moraine, and stratified beds (Kaplan, 1999).

Methods

Study Design and Field Methods

We collected nine paired samples of boulder and bedrock along elevation transects from just above the valley floors to the highest peaks in Acadia National Park, including Cadillac (466 m asl), Sargent (418 m asl), and Pemetic (380 m asl) Mountains (Fig. 2 and 3). Multiple mountains were sampled because we did not find enough suitable co-located boulder and bedrock samples on individual vertical transects.

We also collected six boulder samples from the northern edge of the Jordan Pond moraine in Acadia National Park. These boulders are partially submerged by water along the shore of the pond but protrude 0.5-1.5 m above modern (2015) lake level. Lastly, we sampled seven boulders taller than 1 m from the PRMC; two are from the delta top (PR-14-6 and PR-14-7), one is from the front edge of the delta on a gentle slope (PR-14-1), and four extend outward from PR-14-1 along the top a small moraine ridge less than 1-2

high (PR-14-2 through PR-14-5) (Fig. 4). We resampled a boulder from Davis et al. (2015; PRK-17) as our PR-14-1.

At each sampling site, we targeted surfaces that exhibited characteristics of glacial erosion (e.g., striations and/or polish) to reduce the likelihood of measuring ^{10}Be inherited from prior episodes of exposure and loss of ^{10}Be by erosion since deglaciation. We also sought to avoid boulders on slopes and bedrock with signs of previous soil cover. We recorded latitude and longitude with a handheld GPS, measured topographic shielding using an inclinometer, determined surface orientation with a Brunton compass, photographed boulders, and measured sample thickness as well as boulder dimensions.

Sample Preparation and Isotopic Analysis

Samples were processed at the University of Vermont following the procedures in Corbett et al. (2016). Samples were crushed and pulverized to individual grains, underwent magnetic separation, and non-quartz minerals were removed through etching in weak acid (Kohl and Nishiizumi, 1992). Quartz purity was quantified with inductively coupled plasma optical emission spectrometry. Approximately 225 μg of ^9Be (carrier made from beryl at University of Vermont) was added to each sample. Samples were prepared in three batches each containing one process blank and one CRONUS standard (Standard N; Jull et al., 2015). Beryllium was isolated through anion and cation column chromatography, oxidized, mixed with Nb powder, and pressed into cathodes for measurement. Ratios of $^{10}\text{Be}/^9\text{Be}$ were measured at Lawrence Livermore National Laboratory and were normalized to standard 07KNSTD3110 with an assumed $^{10}\text{Be}/^9\text{Be}$ ratio of 2850×10^{-15} (Nishiizumi et al., 2007). We corrected for background by subtracting the average of three full process blanks ($6.22 \pm 4.91 \times 10^{-16}$, 1SD) from all

sample values and propagated uncertainties in quadrature. Blank-corrected $^{10}\text{Be}/^9\text{Be}$ ratios range from 1.31×10^{-13} to 5.57×10^{-14} .

Exposure Age Calculations

Sample exposure ages were calculated with the CRONUS-Earth online calculator version 2.2 (Balco, 2008) and constants version 2.2.1, using the regional northeastern North American production rate (Balco et al., 2009). The reported ages use the Lal (1991)/Stone (2000) constant production rate model and scaling scheme, though we note that other schemes yield similar ages (to within a century) since the latitude and elevation difference is minimal between the calibration sites and our study area. We assume no post-exposure erosion, no snow cover, a rock density of 2.7 g cm^{-3} , and do not account for production rate changes related to isostatic rebound because these likely would have affected the calibration sites and our study site similarly since they are close in location and age. However, we estimated how much uplift could potentially affect our ages by taking the uplift history of our field site from the ICE-6G model (Peltier et al., 2015) to determine its time-averaged elevation, and using this value to recalculate exposure ages, as done by Cuzzone et al. (2016). This uplift correction would increase exposure ages by ~1%, which is within our reported uncertainty (see supplementary material).

We report the arithmetic mean age for landforms, excluding outliers based on an interquartile range analysis (which considers any value more than 1.5 times outside the difference between the 25th and 75th percentile of the dataset an outlier; Boslaugh, 2012), and quantify uncertainties as the standard error of ages plus the production rate uncertainty, added in quadrature. The close agreement of the northeastern North American production rate and the more precise Arctic production rate (Young et al.,

2013) suggests that our uncertainty estimate may be conservative. We use internal uncertainties when focusing on samples within our dataset, but show external uncertainties when comparing our exposure ages to other paleoclimate records. In order to generate probabilistic estimates of the rate of ice-sheet thinning implied by the Acadia dipstick data, we followed the Monte Carlo approach of Johnson et al. (2014), fitting 1,000 linear regressions through the age-elevation data while randomly varying errors within the uncertainty of the sample age and excluding simulations with negative thinning rates. We ran four sets of Monte Carlo simulations: with the boulder and bedrock population, with just the bedrock, with just the boulders, and with averaged boulder-bedrock pairs (i.e. averaged sample pairs at a given elevation, giving eight groupings), using internal uncertainties in the first three sets and the standard error of sample pairs in the last set to drive the simulation.

Results

Background-corrected sample ^{10}Be concentrations are $3.74\text{-}8.59 \times 10^4$ atoms g^{-1} . Most exposure ages from the Acadia National Park vertical transect (Fig. 5 and 6, Table 1) cluster between 14.5 ± 0.4 and 16.2 ± 0.5 ka, but two boulders (MDI-23, MDI-25) are significantly younger (11.3 ± 0.2 and 12.4 ± 0.2 ka, respectively), perhaps due to rolling, snow/soil cover, or erosion, and are excluded as outliers based on the interquartile range analysis. A paired t -test indicates that there is no significant difference between boulder and bedrock mean ages ($p = 0.24$). Similarly, an independent t -test considering boulder and bedrock samples as two distinct populations also indicates indistinguishable age distributions ($p = 0.15$). The exposure ages are indistinguishable from top to bottom, showing no significant trend with elevation whether considering the full population, the

boulder population alone, the bedrock population alone, or the average of exposure ages at each elevation (Fig. 7). The mean exposure age of the entire dipstick population is 15.2 ± 0.7 ka ($n = 16$). Monte Carlo simulations indicate that the ice sheet surface likely lowered at a rate of decimeters to meters per year (Fig 7e); we note that the Monte Carlo analysis cannot constrain the highest possible thinning rates but is able to place quantitative bounds on the lowest plausible rates.

The Jordan Pond moraine has an average exposure age of 13.3 ± 0.7 ka ($n = 5$), excluding one young outlier MDI-19 (8.9 ± 0.3 ka), and displays a multi-modal distribution (Fig. 6c). The average exposure age of boulders on the PRMC (Fig. 4) is 14.5 ± 0.7 ka ($n = 7$), with ages ranging from 13.9 ± 0.4 to 15.3 ± 0.4 ka (Fig. 6d). The ^{10}Be and ^{26}Al exposure ages from Davis et al. (2015; dashed grey lines in Fig. 6d) on a single boulder from the PRMC have older central tendencies than our age on the same boulder, but they have wide uncertainties that overlap with our data at 1 and 2σ , most likely because extraction methods and measurement precision have improved since the sample of Davis et al. (2015) was analyzed in 2000. The Jordan Pond moraine lies in a stratigraphic position similar to the PRMC, which suggests that both deposits could represent the same stillstand or readvance of the ice. Therefore, we performed a one-way ANOVA, which shows that the ages of the vertical transect in Acadia and the two moraines (Jordan Pond and PRMC) are all separable from each other ($p < 0.001$). This separation indicates that each deposit represents a distinct phase of the coastal deglaciation, presuming the ages are accurate, which we suspect is not the case for the Jordan Pond moraine.

Discussion

¹⁰Be Ages in Coastal Maine

The dipstick exposure ages indicate that the LIS surface lowered in Acadia National Park sometime between 15.5 and 14.5 ka (Fig. 7). These ages are statistically indistinguishable from the rapid thinning identified by Davis et al. (2015) in the Katahdin area of west-central Maine between 16 and 15 ka (*t* test of Acadia ages versus all Katahdin ages, excluding outliers; $p=0.50$), suggesting that ice collapse was regional in scale. The Monte Carlo simulations indicate that thinning occurred in no more than a millennium, and perhaps substantially less, implying thinning rates of decimeters to meters per year (15-680 cm yr⁻¹ at 2 σ ; Fig. 7e). This is broadly comparable to the thinning rates (average = 84 cm yr⁻¹) of the fastest flowing glaciers (>100 m yr⁻¹) in Greenland and the fastest thinning glaciers in Antarctica (9 m yr⁻¹) between 2002 and 2007, which appear to have been driven by dynamic thinning at marine margins (Pritchard et al., 2009).

The Monte Carlo approach we used to quantify thinning rates has been employed in several recent dipstick studies (Johnson et al., 2014; Winsor et al., 2015), but the broad range of possible thinning rates it simulates points to two factors that control the ability of dipsticks to constrain abrupt rates of ice collapse – namely, the precision of the thinning rate will vary as a function of the elevation range spanned by the dipstick relative to the variance of the ages. Thus, all else being equal, the thinning rate distribution will be tighter for taller dipsticks; our study spans only 300 m of relief. Moreover, geologic scatter of cosmogenic ages also tends to bias the result to slower thinning because it allows a wider range of possible thinning rates. For instance, identical ages along a dipstick with zero uncertainty would imply instantaneous thinning, but

wider error bars on the ages would also allow for simulations consistent with more gradual thinning. This limitation could potentially be overcome by averaging multiple ages per elevation to reduce noise. Given that the boulder and bedrock populations from Acadia National Park are indistinguishable – consistent with effective erosion by warm-based ice – we applied this averaging approach, and find that it indeed yields a more monotonic age-elevation relationship than considering the samples individually (Fig. 7d).

Our exposure age for the PRMC, 14.5 ± 0.7 ka, is slightly younger than previous estimates of ~ 16 - 15 cal ka based on radiocarbon constraints that assumed a 400-600 ^{14}C year reservoir correction (Kaplan, 2007). Our PRMC age is also several centuries younger than the nearby Acadia dipstick ages, indicating that the LIS margin may have stabilized at the PRMC as suggested by Thompson and Borns (1985), and perhaps represents an example of the effect of morainal banks on grounding line stability (Alley et al., 2007).

The Jordan Pond moraine age that we obtained of 13.3 ± 0.7 ka is roughly 1,000 years younger than the PRMC and the youngest Acadia dipstick ages (Fig. 6), which is difficult to explain glaciologically because Jordan Pond is outboard of the PRMC and only slightly lower than the bottom of the dipstick. Moreover, the multi-modal distribution of Jordan Pond ages suggests that the boulders do not share a simple history of exposure (Fig. 6c). Several processes may explain why these ages are younger and more scattered than others in our study. Jordan Pond initially drained through its southeast corner following deglaciation, until a new outlet was cut through till to bedrock at the southwest corner of the pond, stabilizing the lake at its current level. LiDAR imagery of the original sluiceway's elevation indicates that the former lake level was ~ 1

m higher than present, which would have shielded the shortest boulder we sampled (MDI-20, 13.4 ka, 0.5 m above lake level) by ~30%, but likely had little to no effect on the four taller boulder samples (1.0-1.5 m, 12.2-14.3 ka), as evidenced by the lack of a relationship between boulder height and age ($r^2 = 0.28$, $p = 0.36$). In addition, the current setting of the boulders on the edge of the moraine, several meters below its crest and partially submerged in lake water, suggests that the boulders may have initially been covered by till before wave action exhumed them. Lastly, deep snow drifts typically accumulate at the southern end of Jordan Pond in modern times during winter, suggesting that snow shielding may further contribute to the young apparent exposure ages of the boulders. Because of these concerns, we consider the Jordan Pond moraine mean exposure age a minimum estimate, though we note that our oldest boulder (14.3 ± 0.3 ka; MDI-17) lines up with the youngest Acadia dipstick ages and may better represent the moraine's age.

Comparison of ^{10}Be and ^{14}C Ages in Coastal Maine

A comparison of the ^{10}Be ages with nearby radiocarbon ages from terrestrial and marine samples reveal similarities and differences. On the one hand, the radiocarbon ages on terrestrial material from the base of cores collected from Sargent Mountain Pond (15.7 ± 0.7 cal ka, Lowell, 1980; 15.7 ± 0.4 cal ka, Norton et al., 2011; Fig. 5) agree well with the Acadia dipstick average exposure age (15.2 ± 0.7 ka), suggesting that vegetation became established rapidly following deglaciation. On the other hand, the ^{10}Be dipstick ages are ~1,000 years younger than the 16.1 ka isochron drawn through Mount Desert Island by Borns et al. (2004; Fig. 1) assuming a 600 ^{14}C year reservoir correction for marine radiocarbon ages. Likewise, previous radiocarbon estimates of the PRMC based

on marine shells assuming a 400-600 ^{14}C year reservoir correction (Kaplan, 2007; 16.1-15.2 cal ka, recalibrated with MARINE13) are slightly older than our mean exposure age on the PRMC (14.5 ± 0.7 ka), and require a 1,200 ^{14}C year marine reservoir correction to be brought into better agreement (15.0-14.0 ka; see supplementary material). These exposure and marine radiocarbon age discrepancies therefore suggest that the deglacial marine reservoir effect was over 1,000 ^{14}C years in coastal Maine, which confirms earlier suggestions of large reservoir ages in this area based on co-existing marine and terrestrial organic material in the Presumpscot Formation at Portland, Maine (Thompson et al., 2011) and varve chronologies of deglaciation to the west (Ridge et al., 2001). However, we note that although our exposure ages are relatively precise (average analytical uncertainty of 2.3%), there is the possibility of a systematic offset if the production rate is incorrect on the order of ± 700 years (i.e., given the 4.8% uncertainty of the northeastern North American production rate), or if all samples have experienced similar histories of snow cover or erosion, which we consider unlikely.

Paleoclimate Implications of LIS deglaciation in Coastal Maine

Our cosmogenic exposure dipstick ages in Acadia National Park (15.2 ± 0.7 ka) indicate that the LIS thinned in coastal Maine during late HS1 (Fig. 8), an association bolstered by several arguments. First, the ^{10}Be production rate is now well anchored in this region with the northeastern North American calibration (Balco et al., 2009), and latitude/elevation scaling uncertainties are minimal since our field site is spatially (≤ 400 km) and temporally (deglacial) close to most of the calibration sites. Second, extensive radiocarbon dating in coastal Maine, perhaps most notably the terrestrial basal ages from Sargent Mountain Pond cores (Norton et al., 2011), also place ice retreat from the coast

during HS1. Lastly, given the multi-millennial duration of HS1, the only other climate interval during which coastal ice retreat plausibly occurred is the Bølling/Allerød after 14.6 ka. However, a Bølling/Allerød age would imply that our exposure ages are too old by upwards of 1,000 years and that marine radiocarbon reservoir corrections would need to be $\geq 2,000$ ^{14}C years, which together seem unlikely.

A more difficult question to answer is why did rapid collapse of the southeastern LIS happen during the cold HS1 interval? We suggest two possible scenarios. The first scenario relies on oceanic heat buildup in the Gulf of Maine due to AMOC weakening. Recent high-resolution climate model simulations that capture details of coastal bathymetry demonstrate a relationship between AMOC weakening and warming in the northwest Atlantic Shelf of several degrees Celsius. These simulations use modern boundary conditions, and thus may not apply to the deglaciation, but they highlight the potential for Atlantic temperature anomalies to be transmitted into the Gulf of Maine via the Northeast Channel (Saba et al., 2015). Furthermore, paleoclimate modeling studies suggest that AMOC weakening during Heinrich stadials produced subsurface warming in the North Atlantic (Alvarez-Solas et al., 2010, 2013; Marcott et al., 2011). Modern melting rates of outlet glaciers around Antarctica show a positive relationship of an extra 1 m per year of basal melt for each 0.1°C ocean temperature increase (Rignot and Jacobs, 2002). Thus, even slight increases in ocean temperatures in the Gulf of Maine could have led to substantially increased sub-ice shelf melting and/or faster calving rates in the marine embayment, which could have increased ice discharge and surface drawdown further upstream. Alternatively, rather than bottom-up oceanic forcing, a second scenario calls on top-down ice sheet melt induced by the atmosphere. Denton et

al. (2005) suggested that HS1 cooling was mainly a winter phenomenon associated with extensive sea ice in the North Atlantic and that summers continued to warm due to rising insolation and CO₂ (Fig. 8), which could have driven an increasingly negative ice surface mass balance over a large portion of the ice sheet surface.

Our PRMC mean age (14.5 ± 0.7 ka) corresponds within uncertainty to the beginning of the Bølling interstadial at 14.6 ka (Rasmussen et al., 2014), suggesting that the LIS may have abandoned the PRMC in response to abrupt warming at the Bølling onset associated with strengthening of the AMOC (Dorion et al., 2001; Borns et al., 2004; Fig. 8). An additional possibility is that the ice margin was forced off of the PRMC by the rapid ~15 m jump in global sea level associated with meltwater pulse 1A that also occurred at this time (14.6-14.3 ka; Deschamps et al., 2012). This sea-level ratcheting would only be plausible if meltwater pulse 1A was largely sourced from Antarctica rather than North America, since the decreased self-gravitation from the shrinking ice sheet would cause a sea-level fall in the near field (Clark et al., 2002).

Our new cosmogenic ages, in the context of previous work (Fig. 1), reveal the broad pattern of deglaciation in Maine. There was slow net retreat in coastal Maine during HS1, punctuated with multiple readvances and stillstands (e.g., PRMC, Pond Ridge moraine), followed by more rapid retreat inland during the Bølling (Borns et al., 2004; Ridge et al., 2004), which was interrupted during the Allerød at 14-13 ka with deposition of the Littleton-Bethlehem and Androscoggin moraines in western Maine/northern New Hampshire (Bromley et al., 2015; Thompson et al., 2017). A similar shift from slower HS1 to accelerated Bølling retreat, both punctuated by shorter events, is

also evident in the Connecticut valley varve record to the west, and suggests that these patterns were at least regional in scale (Ridge et al., 2012).

Conclusions

Sixteen ^{10}Be exposure ages down mountainsides in Acadia National Park are indistinguishable within uncertainty over a 300 m range in elevation, suggesting that the LIS in coastal Maine thinned rapidly at 15.2 ± 0.7 ka during the latter part of HS1, perhaps related to regional oceanic heat buildup or summertime warming. We also provide the first direct and precise dating of the Pineo Ridge moraine complex, with seven boulders yielding a mean exposure age of 14.5 ± 0.7 ka. This later timing suggests that the ice margin stabilized at PRMC for several centuries after the rapid thinning in Acadia, and then resumed retreat coincident within uncertainty of Bølling warming or meltwater pulse 1A sea-level rise. A comparison of these exposure ages to nearby radiocarbon ages indicates that the deglacial marine reservoir effect in this area was $\sim 1,200$ ^{14}C years, considerably higher than many, though not all, previous estimates. This discrepancy suggests caution in interpreting marine radiocarbon ages of deglaciation and isostatic rebound in coastal New England and highlights the potential of cosmogenic dating to improve coastal chronologies in this region.

Acknowledgments

I acknowledge Acadia National Park's permission to sample, help from R. E. Nelson in the field, A. Denn in the lab, and G. Longworth for the digital elevation model of Mount Desert Island. Research supported by National Science Foundation grant EAR-1603175 to Shakun, EAR-1602280 to Bierman, and Boston College startup funds. This is LLNL

paper contribution #707927.

References

- Alley, R.B., Anandakrishnan, S., Dupont, T.K., Parizek, B.R., Pollard, D., 2007. Effect of sedimentation on ice-sheet grounding-line stability. *Science* 315, 1838–1842. doi:10.1126/science.1138396
- Alvarez-Solas, J., Charbit, S., Ritz, C., Paillard, D., Ramstein, G., Dumas, C., 2010. Links between ocean temperature and iceberg discharge during Heinrich events. *Nat. Geosci.* 3, 122–126. doi:10.1038/ngeo752
- Alvarez-Solas, J., Robinson, A., Montoya, M., Ritz, C., 2013. Iceberg discharges of the last glacial period driven by oceanic circulation changes. *Proc. Natl. Acad. Sci. U. S. A.* 110, 16350–4. doi:10.1073/pnas.1306622110
- Andersen, K.K., Azuma, N., Barnola, J.-M., Bigler, M., Biscaye, P., Caillon, N., Chappellaz, J., Clausen, H.B., Dahl-Jensen, D., Fischer, H., Flückiger, J., Fritzsche, D., Fujii, Y., Goto-Azuma, K., Grønvold, K., Gundestrup, N.S., Hansson, M., Huber, C., Hvidberg, C.S., Johnsen, S.J., Jonsell, U., Jouzel, J., Kipfstuhl, S., Landais, a, Leuenberger, M., Lorrain, R., Masson-Delmotte, V., Miller, H., Motoyama, H., Narita, H., Popp, T., Rasmussen, S.O., Raynaud, D., Rothlisberger, R., Ruth, U., Samyn, D., Schwander, J., Shoji, H., Siggard-Andersen, M.-L., Steffensen, J.P., Stocker, T., Sveinbjörnsdóttir, A E., Svensson, A, Takata, M., Tison, J.-L., Thorsteinsson, T., Watanabe, O., Wilhelms, F., White, J.W.C., 2004. High-resolution record of Northern Hemisphere climate extending into the last interglacial period. *Nature* 431, 147–151. doi:10.1038/nature02805
- Ashley, G.M., Boothroyd, J.C., Borns, H.W.J., 1991. Sedimentology of late Pleistocene (Laurentide) deglacial-phase deposits, eastern Maine; An example of a temperate marine grounded ice-sheet margin, in: Anderson, J.B., Ashley, G.M. (Eds.), *Glacial Marine Sedimentation; Paleoclimatic Significance*. Geological Society of America Special Paper 261, Boulder, Colorado, 107–125.
- Balco, G., Briner, J., Finkel, R.C., Rayburn, J.A., Ridge, J.C., Schaefer, J.M., 2009. Regional beryllium-10 production rate calibration for late-glacial northeastern North America. *Quat. Geochronol.* 4, 93–107. doi:10.1016/j.quageo.2008.09.001
- Balco, G., Stone, J.O., Lifton, N.A., Dunai, T.J., 2008. A complete and easily accessible means of calculating surface exposure ages or erosion rates from ^{10}Be and ^{26}Al measurements. *Quat. Geochronol.* 3, 174–195. doi:10.1016/j.quageo.2007.12.001

- Balco, G., Schaefer, J.M., 2006. Cosmogenic-nuclide and varve chronologies for the deglaciation of southern New England. *Quat. Geochronol.* 1, 15–28. doi:10.1016/j.quageo.2006.06.014
- Balco, G., Stone, J.O.H., Porter, S.C., Caffee, M.W., 2002. Cosmogenic-nuclide ages for New England coastal moraines, Martha's Vineyard and Cape Cod, Massachusetts, USA. *Quat. Sci. Rev.* 21, 2127–2135. doi:10.1016/S0277-3791(02)00085-9
- Bard, E., Arnold, M., Mangerud, J., Paterne, M., Labeyrie, L., Duprat, J., Melieres, M.-A., Sonstegaard, E., Duplessy, J.C., 1994. The North Atlantic atmosphere-sea surface ^{14}C gradient during the Younger Dryas climatic event. *Earth Planet. Sci. Lett.* 6, 275–287. doi:10.1016/0012-821X(94)90112-0
- Bard, E., 1988. Correction of accelerator mass spectrometry ^{14}C ages measured in planktonic foraminifera: Paleooceanographic implications. *Paleoceanography* 3, 635–645. doi:10.1029/PA003i006p00635
- Barnhardt, W.A., Belknap, D.F., Kelley, J.T., 1997. Stratigraphic evolution of the inner continental shelf in response to late Quaternary relative sea-level change, northwestern Gulf of Maine. *Bull. Geol. Soc. Am.* 109, 612–630. doi:10.1130/0016-7606(1997)109<0612:SEOTIC>2.3.CO;2
- Bassis, J.N., Walker, C.C., 2012. Upper and lower limits on the stability of calving glaciers from the yield strength envelope of ice. *Proc. R. Soc. A Math. Phys. Eng. Sci.* 468, 913–931. doi:10.1098/rspa.2011.0422
- Belknap, D. F., and Shipp, R.C., 1991, Seismic stratigraphy of glacial marine units, Maine inner shelf, in: Anderson, J.B., Ashley, G.M. (Eds.), *Glacial Marine Sedimentation; Paleoclimatic Significance*. Geological Society of America Special Paper 261, 137–157.
- Bierman, P.R., Davis, P.T., Corbett, L.B., Lifton, N.A., Finkel, R.C., 2015. Cold-based Laurentide ice covered New England's highest summits during the Last Glacial Maximum. *Geology* 43, 1059–1062. doi:10.1130/G37225.1
- Bierman, P.R., Marsella, K.A., Patterson, C., Davis, P.T., Caffee, M., 1999. Mid-Pleistocene cosmogenic minimum-age limits for pre-Wisconsinan glacial surfaces in southwestern Minnesota and southern Baffin Island: A multiple nuclide approach. *Geomorphology* 27, 25–39. doi:10.1016/S0169-555X(98)00088-9
- Boex, J., Fogwill, C., Harrison, S., Glasser, N.F., Hein, A., Schnabel, C., Xu, S., 2013. Rapid thinning of the Late Pleistocene Patagonian Ice Sheet followed migration of the Southern Westerlies. *Sci. Rep.* 3, 1–6. doi:10.1038/srep02118
- Borns Jr., H.W., Doner, L.A., Dorion, C.C., Jacobson, G.L., Kaplan, M.R., Kreutz, K.J., Lowell, T. V., Thompson, W.B., Weddle, T.K., 2004. The deglaciation of Maine,

U.S.A., in: Ehlers, J.E., P.G. (Eds.), Quaternary Glaciations - Extent and Chronology, Part II., 89–109

- Borns, H.W.J., 1985. Changing models of deglaciation in northern New England and adjacent Canada. *Geol. Soc. Am.* 197, 135–138. doi:10.1130/SPE197-p135
- Borns, H.W.J., Hughes, T.J., 1977. The implications of the Pineo Ridge readvance in Maine. *Geogr. Phys. Quat.* 31, 203–206. doi:10.7202/1000272ar
- Boslaugh, S., 2012. *Statistics in a Nutshell*, Second eds. Sebastopol, CA.
- Briner, J.P., Goehring, B.M., Mangerud, J., Svendsen, J.I., 2016. The deep accumulation of ^{10}Be at Utsira, southwestern Norway: Implications for cosmogenic nuclide exposure dating in peripheral ice sheet landscapes. *Geophys. Res. Lett.* 43, 1–9. doi:10.1002/2016GL070100
- Briner, J.P., Miller, G.H., Davis, P.T., Bierman, P.R., Caffee, M., 2003. Last glacial maximum ice sheet dynamics in Arctic Canada inferred from young erratics perched on ancient tors. *Quat. Sci. Rev.* 22, 437–444. doi:10.1016/S0277-3791(03)00003-9
- Bromley, G.R.M., Hall, B.L., Thompson, W.B., Kaplan, M.R., Garcia, J.L., Schaefer, J.M., 2015. Late glacial fluctuations of the Laurentide Ice Sheet in the White Mountains of Maine and New Hampshire, U.S.A. *Quat. Res.* 83, 522–530. doi:10.1016/j.yqres.2015.02.004
- Clark, P.U., Dyke, A.S., Shakun, J.D., Carlson, A.E., Clark, J., Wohlfarth, B., Mitrovica, J.X., Hostetler, S.W., McCabe, A.M., 2009. The Last Glacial Maximum. *Science* 325, 710–714. doi:10.1126/science.1172873
- Clark, P.U., Mitrovica, J.X., Milne, G.A., Tamisiea, M.E., 2002. Sea-level fingerprinting as a direct test for the source of global meltwater pulse 1A. *Science* 295, 2438–2441. doi:10.1126/science.1068797
- Clark, P.U., Marshall, S.J., Clarke, G.K., Hostetler, S.W., Licciardi, J.M., Teller, J.T., 2001. Freshwater forcing of abrupt climate change during the last glaciation. *Science* 293, 283–287. doi:10.1126/science.1062517
- Corbett, L.B., Bierman, P.R., Stone, B.D., Caffee, M.W., Larson, P.L., 2017. Cosmogenic nuclide age estimates for Laurentide Ice Sheet recession from the terminal moraine, New Jersey, USA, and constraints on Latest Pleistocene ice sheet behavior: *Quaternary Research*. doi: 10.1017/qua.2017.11
- Corbett, L.B., Bierman, P.R., Rood, D.H., 2016. An approach for optimizing in situ cosmogenic ^{10}Be sample preparation. *Quat. Geochronol.* 33, 24–34. doi:10.1016/j.quageo.2016.02.001

- Corbett, L.B., Bierman, P.R., Graly, J.A., Neumann, T.A., Rood, D.H., 2013. Constraining landscape history and glacial erosivity using paired cosmogenic nuclides in Upernavik, northwest Greenland. *Bull. Geol. Soc. Am.* 125, 1539–1553. doi:10.1130/B30813.1
- Corbett, L.B., Young, N.E., Bierman, P.R., Briner, J.P., Neumann, T.A., Rood, D.H., Graly, J.A., 2011. Paired bedrock and boulder ¹⁰Be concentrations resulting from early Holocene ice retreat near Jakobshavn Isfjord, western Greenland. *Quat. Sci. Rev.* 30, 1739–1749. doi:10.1016/j.quascirev.2011.04.001
- Crossen, K.J., 1991. Structural control of deposition by Pleistocene tidewater glaciers, Gulf of Maine, in: Anderson, J.B., Ashley, G.M. (Eds.), *Glacial Marine Sedimentation; Paleoclimatic Significance*. Geological Society of America Special Paper 261, 127–135.
- Cuzzone, J.K., Clark, P.U., Carlson, A.E., Ullman, D.J., Rinterknecht, V.R., Milne, G.A., Lunkka, J.P., Wohlfarth, B., Marcott, S.A., Caffee, M., 2016. Final deglaciation of the Scandinavian Ice Sheet and implications for the Holocene global sea-level budget. *Earth Planet. Sci. Lett.* 448, 34–41. doi:10.1016/j.epsl.2016.05.019
- Davis, P.T., Bierman, P.R., Corbett, L.B., Finkel, R.C., 2015. Cosmogenic exposure age evidence for rapid Laurentide deglaciation of the Katahdin area, west-central Maine, USA, 16 to 15 ka. *Quat. Sci. Rev.* 116, 95–105. doi:10.1016/j.quascirev.2015.03.021
- Davis, P.T., Davis, R.B., 1980. Interpretation of minimum-limiting radiocarbon dates for deglaciation of Mount Katahdin area, Maine. *Geology* 8, 396–400. doi:10.1130/0091-7613(1980)8<396:IOMRDF>2.0.CO;2
- Deconto, R.M., Pollard, D., 2016. Contribution of Antarctica to past and future sea-level rise. *Nature* 531, 591–597. doi:10.1038/nature17145
- Denton, G.H., Alley, R.B., Comer, G.C., Broecker, W.S., 2005. The role of seasonality in abrupt climate change. *Quat. Sci. Rev.* 24, 1159–1182. doi:10.1016/j.quascirev.2004.12.002
- Deschamps, P., Durand, N., Bard, E., Hamelin, B., Camoin, G., Thomas, A.L., Henderson, G.M., Okuno, J., Yokoyama, Y., 2012. Ice-sheet collapse and sea-level rise at the Bølling warming 14,600 years ago. *Nature* 483, 559–564. doi:10.1038/nature10902
- Dorion, C.C., Balco, G.A., Kaplan, M.R., Kreutz, K.J., Wright, J.D., Borns, H.W., 2001. Stratigraphy, paleoceanography, chronology, and environment during deglaciation of eastern Maine, in: Weddle, T.K., Retelle, M.J. (Eds.), *Deglacial History and Relative Sea-Level Changes, Northern New England and Adjacent Canada.*, 215–242

- Dyke, A.S., 2004. An outline of the deglaciation of North America with emphasis on central and northern Canada. *Quaternary Glaciations-Extent and Chronology Part II North America 2b*, 373–424. doi:10.1016/S1571-0866(04)80209-4
- Dyke, A.S., Moore, A., and Robertson, L., 2003. Deglaciation of North America. Geological Survey of Canada Open File, 1574. Thirty-two digital maps at 1:7,000,000 scale with accompanying digital chronological database and one poster (two sheets) with full map series
- Gilman, R.A., Chapman, C.A., Lowell, T. V., Borns Jr., H.W., 1988. *The Geology of Mount Desert Island - A Visitor's Guide to the Geology of Acadia National Park*. Maine Geological Survey, Department of Conservation, 50 p.
- Goehring, B.M., Brook, E.J., Linge, H., Raisbeck, G.M., Yiou, F., 2008. Beryllium-10 exposure ages of erratic boulders in southern Norway and implications for the history of the Fennoscandian Ice Sheet. *Quat. Sci. Rev.* 27, 320–336. doi:10.1016/j.quascirev.2007.11.004
- Gomez, N., Pollard, D., Holland, D., 2015. Sea-level feedback lowers projections of future Antarctic Ice-Sheet mass loss. *Nat. Commun.* 53, 1–8. doi:10.1017/CBO9781107415324.004
- Gosse, J.C., Phillips, F.M., 2001. Terrestrial in situ cosmogenic nuclides: theory and application. *Quat. Sci. Rev.* 20, 1475–1560. doi:10.1016/S0277-3791(00)00171-2
- Graham, J. 2010, *Acadia National Park: Geologic Resources Inventory Report*. Natural Resource Report NPS/NRPC/GRD/NRR—2010/232. National Park Service, Ft. Collins, Colorado.
- Grimm, E.C., Maher, L.J., Nelson, D.M., 2009. The magnitude of error in conventional bulk-sediment radiocarbon dates from central North America. *Quat. Res.* 72, 301–308. doi:10.1016/j.yqres.2009.05.006
- Heyman, J., Stroeven, A.P., Harbor, J.M., Caffee, M.W., 2011. Too young or too old: Evaluating cosmogenic exposure dating based on an analysis of compiled boulder exposure ages. *Earth Planet. Sci. Lett.* 302, 71–80. doi:10.1016/j.epsl.2010.11.040
- Hughes, T.J., Borns Jr., H.W., Fastook, J.L., Hyland, M.R., Kite, J.S., Lowell, T. V., 1985. Models of glacial reconstruction and deglaciation applied to Maritime Canada and New England, in: Borns Jr., H.W., LaSalle, P., Thompson, W.B. (Eds.), *Late Pleistocene History of Northeastern New England and Adjacent Quebec*. The Geological Society of America, Inc., Boulder, Colorado, 139–150
- Hunter, L.E., Smith, G.W., 2001. Morainal banks and the deglaciation of coastal Maine, in: *Deglacial History and Relative Sea-Level Changes, Northern New England and Adjacent Canada*. Geological Society of America Special Paper 261, 151–170

- Johnson, J.S., Bentley, M.J., Smith, J. A, Finkel, R.C., Rood, D.H., Gohl, K., Balco, G., Larter, R.D., Schaefer, J.M., 2014. Rapid thinning of Pine Island Glacier in the early Holocene. *Science* 343, 999–1001. doi:10.1126/science.1247385
- Joughin, I., Alley, R.B., 2011. Stability of the West Antarctic ice sheet in a warming world. *Nat. Geosci.* 4, 506–513. doi:10.1038/ngeo1194
- Jull, A.J.T., Scott, E.M., Bierman, P., 2015. The CRONUS-Earth inter-comparison for cosmogenic isotope analysis *Quat. Geochronol.* 26, 3–10. doi:10.1016/j.quageo.2013.09.003
- Kaplan, M.R., 2007. Major ice sheet response in eastern New England to a cold North Atlantic region, ca. 16–15 cal ka BP. *Quat. Res.* 68, 280–283. doi:10.1016/j.yqres.2007.06.003
- Kaplan, M.R., 1999. Retreat of a tidewater margin of the Laurentide ice sheet in eastern coastal Maine between ca. 14 000 and 13 000 14C yr B.P. *Geological Society of America Bulletin* 111, 620–632. doi:10.1130/0016-7606(1999)111<0620:ROATMO>2.3.CO;2
- Kelley, J.T., Belknap, D.F., Claesson, S., 2010. Drowned coastal deposits with associated archaeological remains from a sea-level “slowstand”: Northwestern Gulf of Maine, USA. *Geology* 38, 695–698. doi:10.1130/G31002.1
- Kohl, C.P., Nishiizumi, K., 1992. Chemical isolation of quartz for measurement of in-situ-produced cosmogenic nuclides. *Geochim. Cosmochim. Acta* 56, 3583–3587. doi:10.1016/0016-7037(92)90401-4
- Koteff, C., Pessl, F., 1981. Systematic Ice Retreat in New England. *Geologic Survey Professional Paper* 1179, 1–20.
- Lal, D., 1991. Cosmic ray labeling of erosion surfaces: in situ nuclide production rates and erosion models. *Earth Planet. Sci. Lett.* 104, 424–439. doi:10.1016/0012-821X(91)90220-C
- Laskar, J., Robutel, P., Joutel, F., Gastineau, M., Correia, A.C.M., Levrard, B., 2004. A long-term numerical solution for the insolation quantities of the Earth. *Astron. Astrophys.* 428, 261–285. doi:10.1051/0004-6361:20041335
- Lepage, C.A., 1982, The composition and origin of the Pond Ridge moraine, Washington County, Maine [M.S. thesis]: Orono, University of Maine, 124 p.
- Lowell, T.V., 1980, Late Wisconsin ice extent in Maine, evidence from Mt. Desert Island and the St. John River area (M.S. thesis): Orono, University of Maine, 180 p.

- Mangerud, J., 1972. Radiocarbon dating of marine shells, including a discussion of apparent age of Recent shells from Norway. *Boreas* 1, 143–172.
- Marcott, S. A, Clark, P.U., Padman, L., Klinkhammer, G.P., Springer, S.R., Liu, Z., Otto-Bliesner, B.L., Carlson, A.E., Ungerer, A., Padman, J., He, F., Cheng, J., Schmittner, A., 2011. Ice-shelf collapse from subsurface warming as a trigger for Heinrich events. *Proc. Natl. Acad. Sci. U. S. A.* 108, 13415–13419. doi:10.1073/pnas.1104772108
- Marsella, K. A., Bierman, P.R., Thompson Davis, P., Caffee, M.W., 2000. Cosmogenic ^{10}Be and ^{26}Al ages of the Last Glacial Maximum, Eastern Baffin Island, Arctic Canada. *Bull. Geol. Soc. Am.* 112, 1296–1312. doi:10.1130/0016-7606(2000)112<1296:CBAAAF>2.0.CO;2
- McManus, J.F., Francois, R., Gherardi, J.-M., Keigwin, L.D., Brown-Leger, S., 2004. Collapse and rapid resumption of Atlantic meridional circulation linked to deglacial climate changes. *Nature* 428, 834–837. doi:10.1038/nature02494
- NGRIP dating group, 2006, Greenland Ice Core Chronology 2005 (GICC05), IGBP PAGES/World Data Center for Paleoclimatology Data Contribution Series # 2006-118, NOAA/NCDC Paleoclimatology Program, Boulder CO, USA.
- Nishiizumi, K., Imamura, M., Caffee, M.W., Southon, J.R., Finkel, R.C., McAninch, J., 2007. Absolute calibration of ^{10}Be AMS standards. *Nucl. Instruments Methods Phys. Res. Sect. B Beam Interact. with Mater. Atoms* 258, 403–413. doi:10.1016/j.nimb.2007.01.297
- Norton, S.A., Perry, R.H., Saros, J.E., 2011. The controls on phosphorus availability in a Boreal lake ecosystem since deglaciation. *J. Paleolimnol.* 46, 107–122. doi:10.1007/s10933-011-9526-9
- Peltier, W.R., Argus, D.F., Drummond, R., 2015. Space geodesy constrains ice-age terminal deglaciation: The global ICE-6G_C (VM5a) model. *J. Geophys. Res. Solid Earth* 120, 450–487. doi:10.1002/2014JB011176.
- Pfeffer, W.T., Harper, J.T., O’Neel, S., 2008. Kinematic constraints on glacier contributions to 21st-century sea-level rise. *Science* 321, 1340–1343. doi:10.1126/science.1159099
- Pratt, R.M., Schlee, J., 1969. Glaciation on the Continental Margin off New England. *Geol. Soc. Am. Bull.* 80, 2335–2342. doi:10.1130/0016-7606(1969)80[2335:GOTCMO]2.0.CO;2
- Pritchard, H.D., Ligtenberg, S.R.M., Fricker, H.A., Vaughan, D.G., Broeke, M.R. Van Den, Padman, L., 2012. Antarctic ice-sheet loss driven by basal melting of ice shelves. *Nature* 484, 502–505. doi:10.1038/nature10968

- Pritchard, H.D., Arthern, R.J., Vaughan, D.G., Edwards, L.A., 2009. Extensive dynamic thinning on the margins of the Greenland and Antarctic ice sheets. *Nature* 461, 971–975. doi:10.1038/nature08471
- Rasmussen, S.O., Bigler, M., Blockley, S.P., Blunier, T., Buchardt, S.L., Clausen, H.B., Cvijanovic, I., Dahl-Jensen, D., Johnsen, S.J., Fischer, H., Gkinis, V., Guillevic, M., Hoek, W.Z., Lowe, J.J., Pedro, J.B., Popp, T., Seierstad, I.K., Steffensen, J.P., Svensson, A.M., Vallelonga, P., Vinther, B.M., Walker, M.J.C., Wheatley, J.J., Winstrup, M., 2014. A stratigraphic framework for abrupt climatic changes during the Last Glacial period based on three synchronized Greenland ice-core records: Refining and extending the INTIMATE event stratigraphy. *Quat. Sci. Rev.* 106, 14–28. doi:10.1016/j.quascirev.2014.09.007
- Retelle, M.J., Weddle, T.K., 2001. Deglaciation and relative sea-level chronology, Casco Bay Lowland and lower Androscoggin River valley, Maine, in: Weddle, T.K., Retelle, M.J. (Eds.), *Deglacial History and Relative Sea-Level Changes, Northern New England and Adjacent Canada*, 191–214.
- Ridge, J.C., Balco, G., Bayless, R.L., Beck, C.C., Carter, L.B., Dean, J.L., Voytek, E.B., Wei, J.H., 2012. The new North American Varve Chronology: A precise record of southeastern Laurentide Ice Sheet deglaciation and climate, 18.2–12.5 kyr BP, and correlations with Greenland ice core records. *Am. J. Sci.* 312, 685–722. doi:10.2475/07.2012.01
- Ridge, J.C., 2004. The Quaternary glaciation of western New England with correlations to surrounding areas, in: Ehlers, J., Gbbard, P.L. (Eds.), *Quaternary Glaciations - Extent and Chronology, Part II*, 169–199.
- Ridge, J.C., Canwell, B.A., Kelly, M.A., Kelley, S.Z., 2001. Atmospheric ^{14}C chronology for late Wisconsinan deglaciation and sea-level in eastern New England using varve and paleomagnetic records, in: *Deglacial History and Relative Sea-Level Changes, Northern New England and Adjacent Canada: Boulder, Colorado. Geological Society of America Special Paper 351*, 171–189.
- Rignot, E., Jacobs, S.S., 2002. Rapid bottom melting widespread near Antarctic Ice Sheet grounding lines. *Science* 296, 2020–2023. doi:10.1126/science.1070942
- Saba, V.S., Griffies, S.M., Anderson, W.G., Winton, M., Alexander, M.A., Delworth, T.L., Hare, J.A., Harrison, M.J., Rosati, A., Vecchi, G.A., 2015. Enhanced warming of the Northwest Atlantic Ocean under climate change. *J. Geophys. Res. Ocean.* 120, 1–15. doi:10.1002/2015JC011346.Received
- Scambos, T.A., Bohlander, J.A., Shuman, C.A., Skvarca, P., 2004. Glacier acceleration and thinning after ice shelf collapse in the Larsen B embayment, Antarctica. *Geophys. Res. Lett.* 31, 2001–2004. doi:10.1029/2004GL020670

- Schildgen, T.F., Phillips, W.M., Purves, R.S., 2005. Simulation of snow shielding corrections for cosmogenic nuclide surface exposure studies. *Geomorphology* 64, 67–85. doi:10.1016/j.geomorph.2004.05.003
- Schnitker, D., Belknap, D.F., Bacchus, T.S., Friez, J.K., Lusardi, B.A., and Popek, D.M., 2001, Deglaciation of the Gulf of Maine, in: Weddle, T. K., and Retelle, M.J., eds., *Deglacial History and Relative Sea-Level Changes, Northern New England and Adjacent Canada*: Boulder, Colorado, Geological Society of America Special Paper 351, p. 9–34
- Schoof, C., 2007. Ice sheet grounding line dynamics: Steady states, stability, and hysteresis. *J. Geophys. Res.* 112, 1–19. doi:10.1029/2006JF000664
- Smith, G.W., 1985. Chronology of Late Wisconsinan deglaciation of coastal Maine, in: Borns Jr., H.W., LaSalle, P., Thompson, W.B. (Eds.), *Late Pleistocene History of Northeastern New England and Adjacent Quebec*. The Geological Society of America Special Paper 197, 29–44.
- Stone, J.O., Balco, G. A, Sugden, D.E., Caffee, M.W., Sass, L.C., Cowdery, S.G., Siddoway, C., 2003. Holocene deglaciation of Marie Byrd Land, West Antarctica. *Science* 299, 99–102. doi:10.1126/science.1077998
- Stone, J.O., 2000. Air pressure and cosmogenic isotope production. *J. Geophys. Res.* 105, 753–759. doi:10.1029/2000JB900181
- Straneo, F., Heimbach, P., 2013. North Atlantic warming and the retreat of Greenland’s outlet glaciers. *Nature* 504, 36–43. doi:10.1038/nature12854
- Stuiver, M., Reimer, P.J., and Reimer, R.W., 2016, CALIB 7.1 [WWW program] at <http://calib.org>, accessed 2016-6-20
- Stuiver, M., Pearson, G.W., Braziunas, T., 1986. Radiocarbon age calibrate of marine samples back to 9000 cal yr BP. *Radiocarbon* 28, 980–1021. doi:10.1017/S0033822200060264
- Stuiver, M., Borns, H.W., 1975. Late quaternary Marine invasion in Maine: Its chronology and associated crustal movement. *Bull. Geol. Soc. Am.* 86, 99–104. doi:10.1130/0016-7606(1975)86<99:LQMIIM>2.0.CO;2
- Thompson, W.B., Dorion, C.C., Ridge, J.C., Balco, G., Fowler, B.K., Svendsen, K.M., 2017. Deglaciation and late-glacial climate change in the White Mountains, New Hampshire, USA. *Quat. Res.* 87, 96–120. doi:10.1017/qua.2016.4
- Thompson, W.B., 2015. *Surficial Geology Handbook for Southern Maine*. Maine Geological Survey, Department of Conservation, 97 p.

- Thompson, W.B., Griggs, C.B., Miller, N.G., Nelson, R.E., Weddle, T.K., Kilian, T.M., 2011. Associated terrestrial and marine fossils in the late-glacial Presumpscot Formation, southern Maine, USA, and the marine reservoir effect on radiocarbon ages. *Quat. Res.* 75, 552–565. doi:10.1016/j.yqres.2011.02.002
- Thompson, W.B., Fowler, B.K., Dorion, C.C., 1999. Deglaciation of the Northwestern White Mountains, New Hampshire. *Géographie Phys. Quat.* 53, 59–77. doi:10.7202/004882ar
- Thompson, W.B., Crossen, K.J., Andersen, B.G., 1989. Glaciomarine Deltas of Maine and Their Relation to Late Pleistocene-Holocene Crustal Movements, in: Andersen, W. A., and Borns Jr., H.W., (Ed.), *Neotectonics of Maine; Studies in Seismicity, Crustal Warping, and Sea-Level Change*. Maine Geological Survey, Augusta, pp. 43–67.
- Thompson, W.B., Borns Jr., H.W., 1985. Till stratigraphy and Late Wisconsinan deglaciation of southern Maine: A Review. *Géographie Phys. Quat.* 39, 199. doi:10.7202/032602ar
- Thornalley, D.J.R., McCave, I.N., Elderfield, H., 2010. Freshwater input and abrupt deglacial climate change in the North Atlantic. *Paleoceanography* 25, 1–16. doi:10.1029/2009PA001772f
- Tucholke, B.E., Hollister, C.D., 1973. Late Wisconsin Glaciation of the Southwestern Gulf of Maine: New evidence from the Marine Environment. *Geol. Soc. Am. Bull.* 84, 3279–3296. doi:10.1130/0016-7606(1973)84<3279:LWGOTS>2.0.CO;2
- Ullman, D.J., Carlson, A. E., LeGrande, A. N., Anslow, F.S., Moore, A. K., Caffee, M., Syverson, K.M., Licciardi, J.M., 2014. Southern Laurentide ice-sheet retreat synchronous with rising boreal summer insolation. *Geology* 43, 23–26. doi:10.1130/G36179.1
- U.S. Geological Survey, 2013, USGS NED n45w068 1/3 arc-second 2013 1 x 1 degree ArcGrid: U.S. Geological Survey: Reston, VA, <http://ned.usgs.gov/>, <http://nationalmap.gov/viewer.html>.
- Waelbroeck, C., Duplessy, J.C., Michel, E., Labeyrie, L., Paillard, D., Duprat, J., 2001. The timing of the last deglaciation in North Atlantic climate records. *Nature* 412, 724–727. doi:10.1038/35106623
- Winsor, K., Carlson, A.E., Caffee, M.W., Rood, D.H., 2015. Rapid last-deglacial thinning and retreat of the marine-terminating southwestern Greenland ice sheet. *Earth Planet. Sci. Lett.* 426, 1–12. doi:10.1016/j.epsl.2015.05.040
- Young, N.E., Schaefer, J.M., Briner, J.P., Goehring, B.M., 2013. A ^{10}Be production-rate calibration for the Arctic. *J. Quat. Sci.* 28, 515–526. doi:10.1002/jqs.2642.

Figures

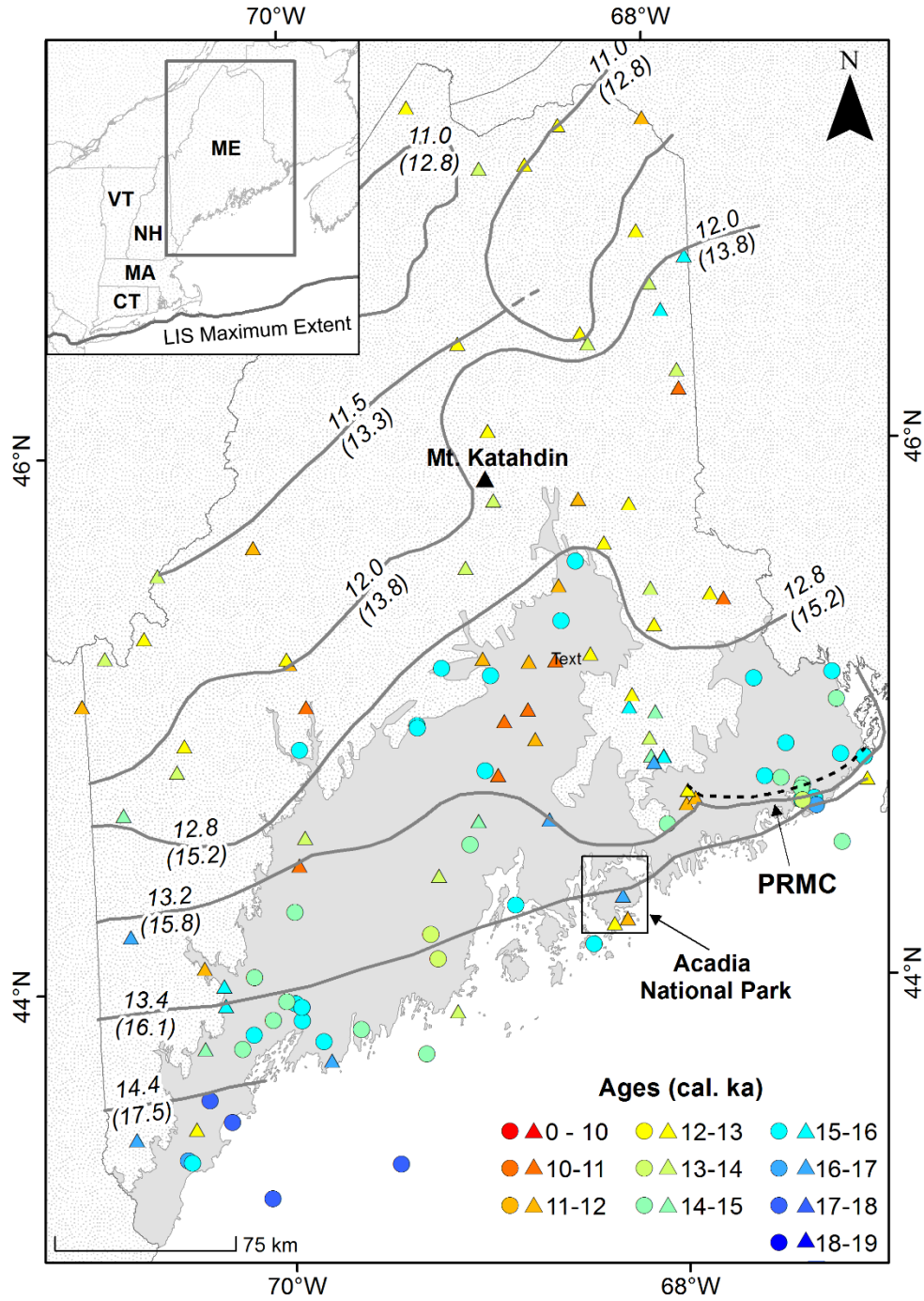


Figure 1: Deglaciation in Maine. Calibrated radiocarbon ages that constrain deglaciation throughout Maine from Dyke et al. (2003). Terrestrial samples (triangles) were calibrated with IntCal13, and marine samples (circles) were calibrated with MARINE13 using the built-in reservoir correction of 405 years (Stuiver et al., 2016). The shaded grey zone depicts the area of postglacial marine submergence. The isochrons are based on Fig. 1 in Borns (2004) with reservoir

correction of 600 ^{14}C years, and show radiocarbon ages followed by calibrated ages in parentheses. The inset map shows the location of Maine within New England and the LGM margin of the LIS as thick black line. PRMC = Pineo Ridge moraine complex, indicated by dashed line. The black box shows the location of Fig. 3. Full radiocarbon data are provided in Table 1 in the supplementary material.



Figure 2: Sample examples. Photographs of boulder and bedrock samples from the **(a)** Jordan Pond moraine (MDI-20), **(b)** Acadia National Park vertical transect (MDI-06 (bedrock in rear) and MDI-05 (boulder in foreground)), and **(c)** Pineo Ridge moraine complex (PR-14-4 (boulder on left) and PR-14-5 (boulder on right)).

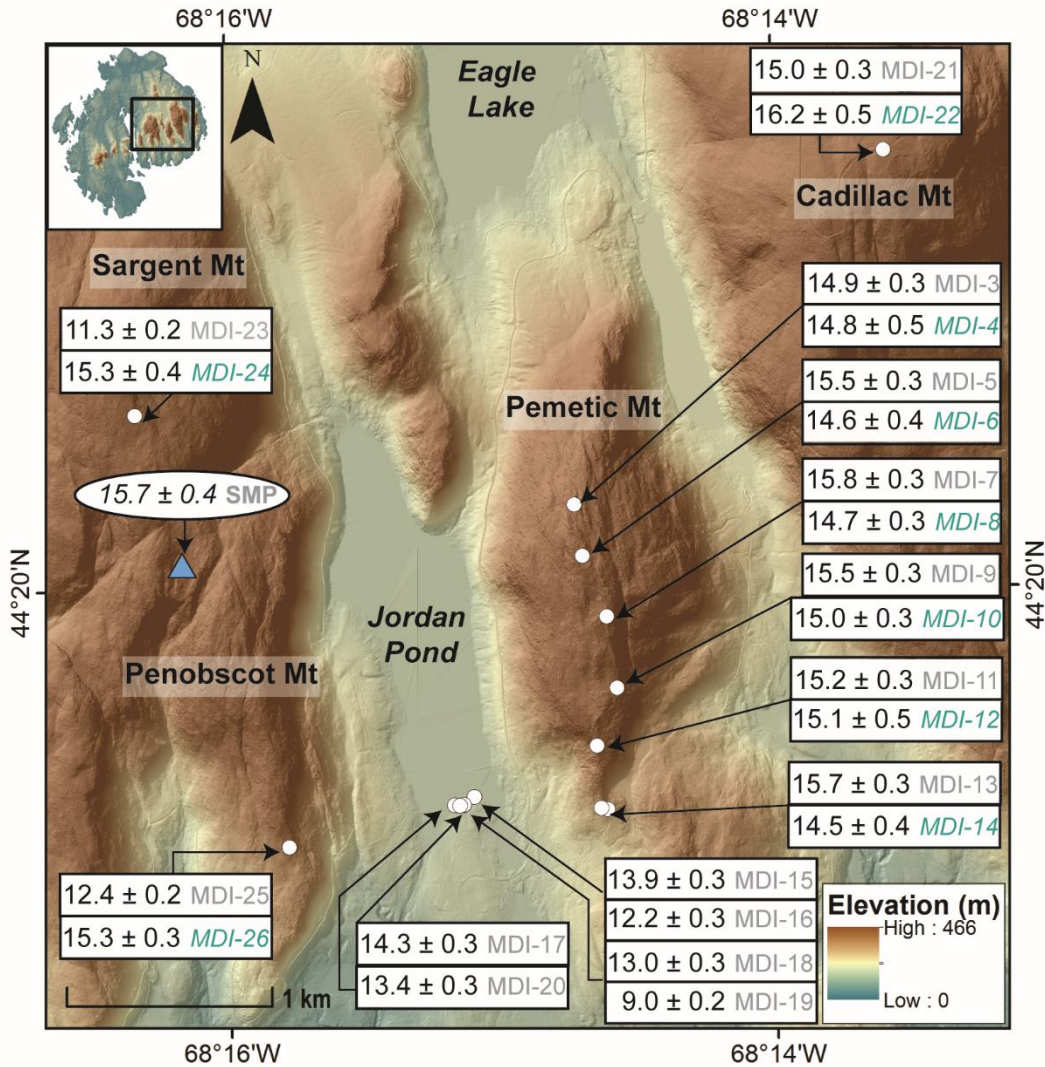


Figure 3: Map of Acadia National Park. A LiDAR digital elevation model with a transparent hillshade of Mount Desert Island showing ¹⁰Be exposure ages with 1σ internal uncertainties (in ka) in Acadia National Park. The calibrated basal radiocarbon age from a Sargent Mountain Pond sediment core (SMP) is shown for comparison (Norton, et al., 2011). Boulder ages are gray and bedrock ages are italicized green. Full exposure age data are provided in Table 1 and Supplementary Table 2. (LiDAR data from Gordon Longsworth, pers. comm.).

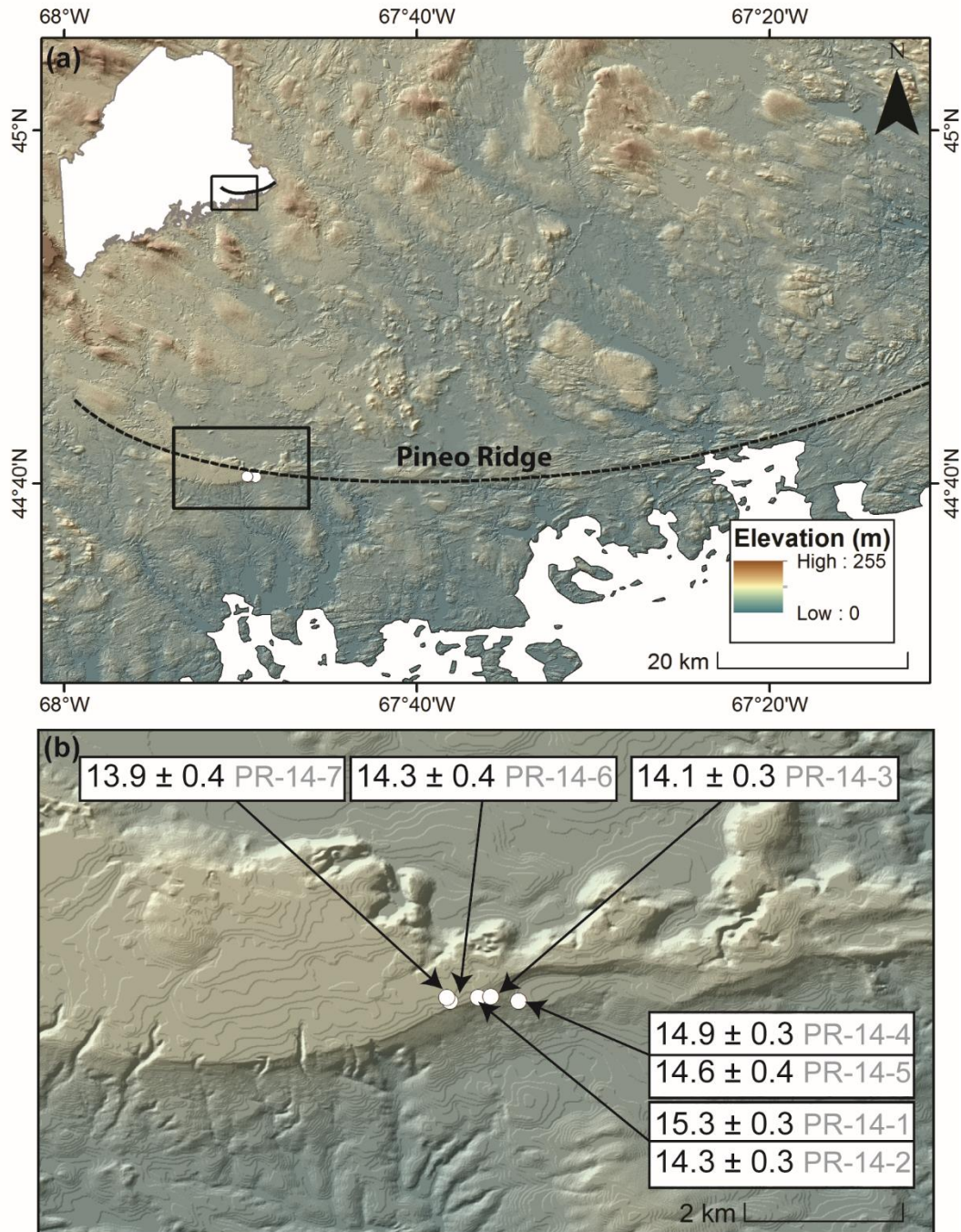


Figure 4: Map of the Pineo Ridge moraine complex (a) A 1/3 arcsecond LiDAR digital elevation model (USGS, 2013) with a transparent hillshade showing the location of the Pineo Ridge moraine complex in coastal Maine (black dashed line). Sample locations are represented by white dots. The black line on the Maine inset shows the location of PRMC. Black box shows the

location of panel b. **(b)** ^{10}Be ages with 1σ internal uncertainty (in ka) of seven boulders on Pineo Ridge. Full exposure age data are provided in Table 1 and Supplementary Table 2.

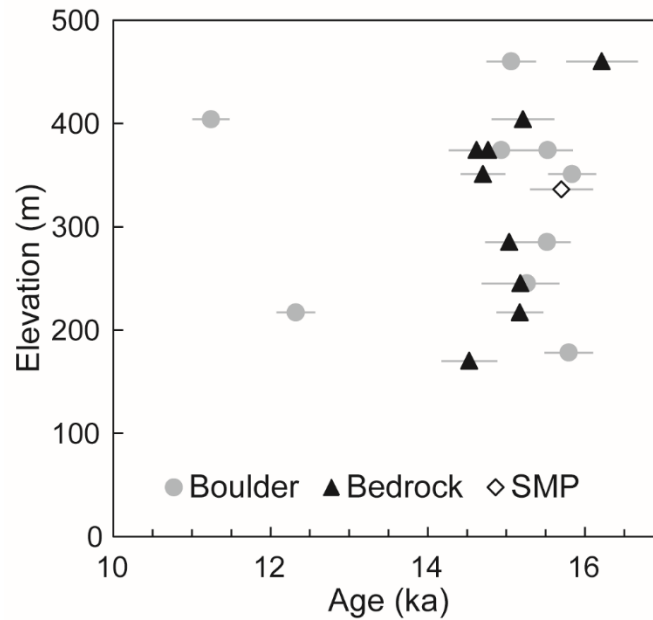


Figure 5: Exposure ages in Acadia National Park. ^{10}Be ages of boulder (circles) and bedrock (triangles) sample pairs taken at the same elevations from Acadia National Park. Calibrated basal radiocarbon age from Sargent Mountain Pond (SMP, Fig. 3) is the open diamond (Norton et al., 2011). Error bars show 1σ internal uncertainty.

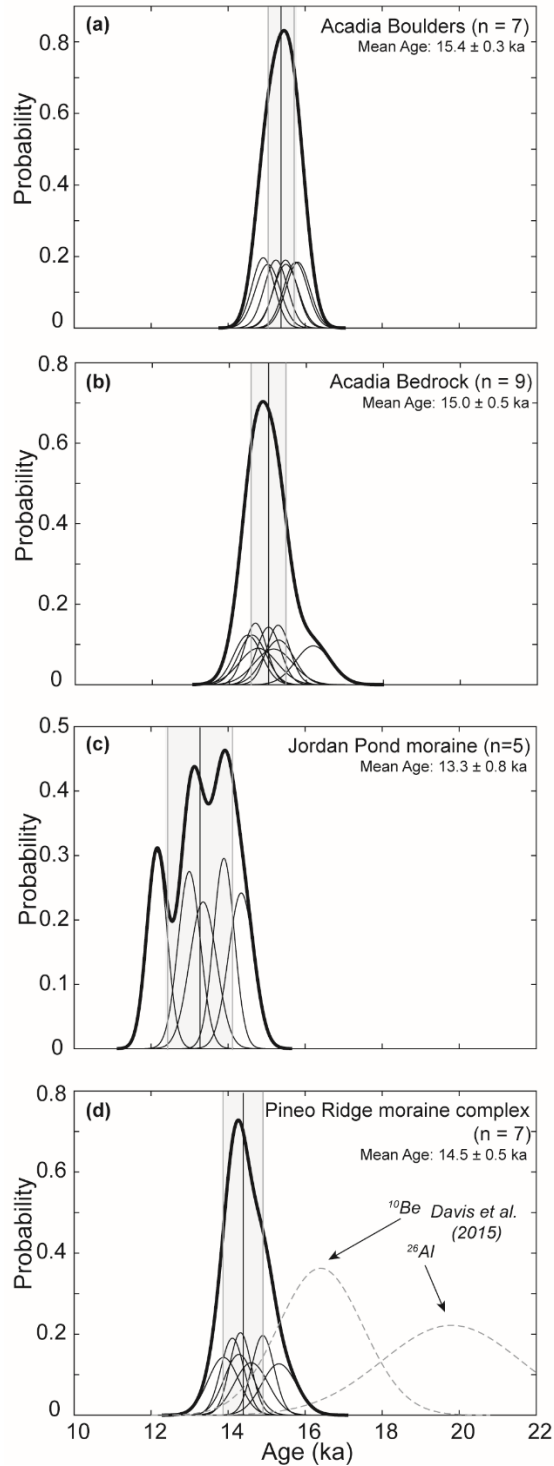


Figure 6: Probability distribution functions (camel plots) of ^{10}Be ages. (a) Acadia National Park boulders, **(b)** Acadia National Park bedrock, **(c)** Jordan Pond moraine boulders, and **(d)** Pineo Ridge moraine complex boulders. Thin lines represent individual samples with internal uncertainties, and thick black lines show summed probability distributions. The plots exclude two Acadia boulder outliers (MDI-23, MDI-25) and one Jordan Pond outlier (MDI-19). The two grey

dashed lines in panel d represent the ^{10}Be and ^{26}Al ages from Davis et al. (2015) on a Pineo Ridge moraine complex boulder (PTK-17), resampled for this study. Vertical gray bars show mean age and standard deviation.

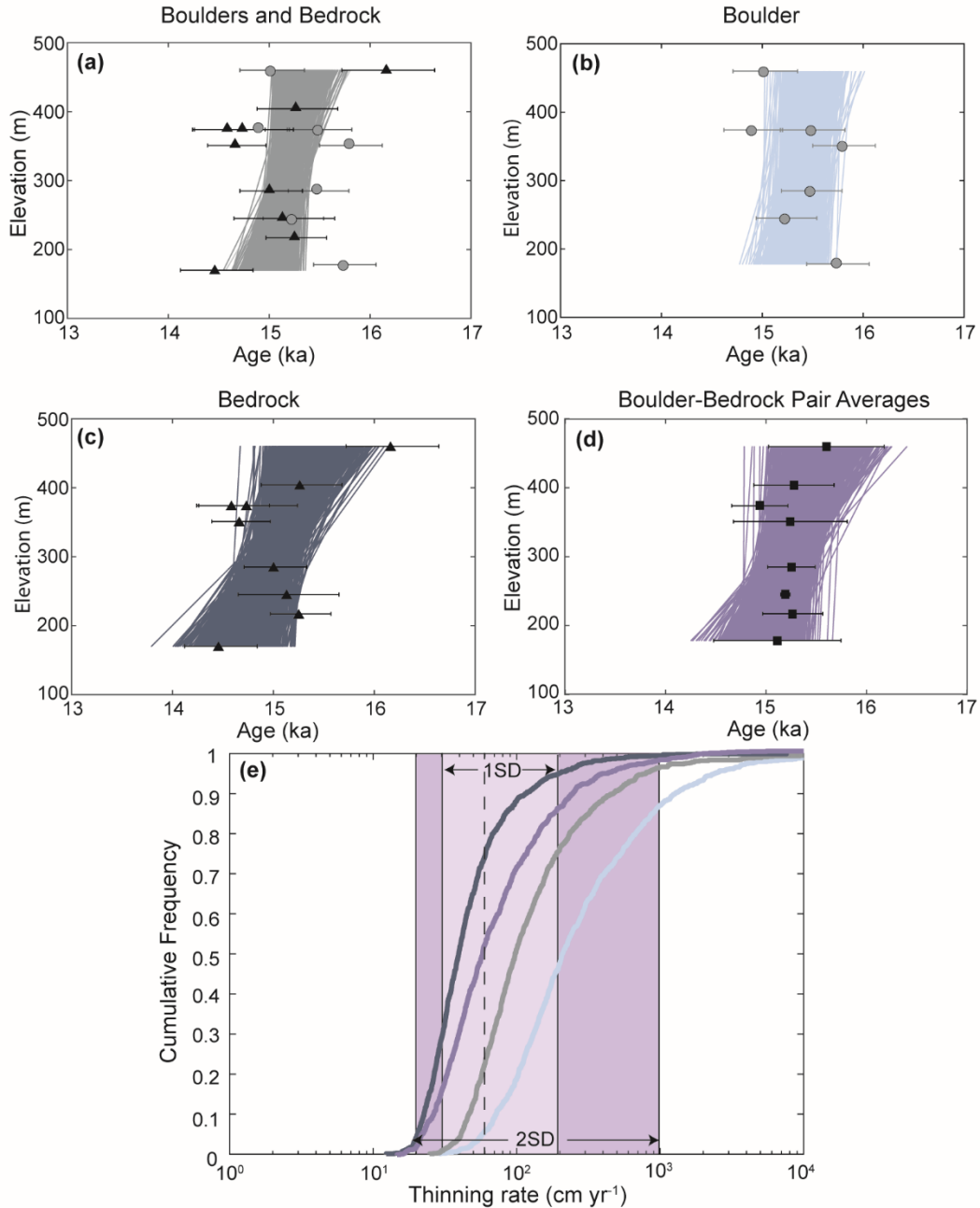


Figure 7: Monte Carlo Analysis. ^{10}Be ages from Acadia National Park with 1000 age-elevation regressions (Johnson et al., 2014) generated by randomly resampling boulders (grey circles) and bedrock (black triangles) ages across their uncertainty ranges (considering internal rather than external uncertainties, since production rate and scaling uncertainties are common to all samples).

Two outlier boulder samples are excluded (MDI-23, MDI-25). Age-elevation regressions using **(a)** boulder and bedrock data, **(b)** boulders, **(c)** bedrock, and **(d)** boulder-bedrock pair averages at each elevation. We prefer model d since averaging produces a more monotonic age-elevation relationship than considering boulders and bedrock separately. Error bars show 1σ internal uncertainty in panels a-c, and standard error of boulder-bedrock pairs in panel d. **(e)** Cumulative frequency curves of the thinning rates implied by the regressions shown in panels a-d, and colored accordingly. The purple bars represent the 1 and 2 standard deviation range of the thinning rates from the boulder-bedrock pair averages.

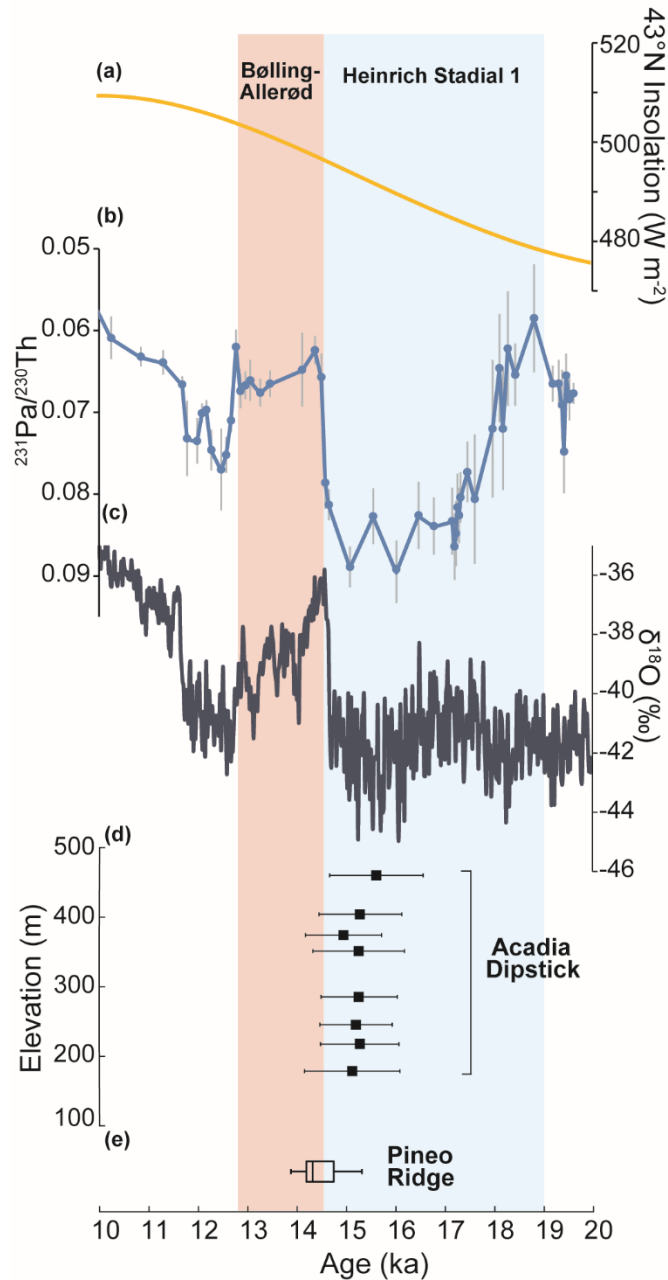


Figure 8: Paleoclimate records from the Northern Hemisphere compared to Acadia ^{10}Be dipstick ages. (a) 43°N June insolation curve (Laskar et al., 2004), (b) North Atlantic sediment $^{231}\text{Pa}/^{230}\text{Th}$, a proxy for Atlantic Meridional Overturning Circulation strength (McManus et al., 2004), (c) Greenland ice core $\delta^{18}\text{O}$ (NGRIP dating group, 2006) a proxy for North Atlantic temperature, (d) ^{10}Be dipstick ages of boulder-bedrock pair averages and the Pineo Ridge moraine complex age, with uncertainties combining the standard error of ages and the production rate uncertainty (4.8%) added in quadrature, (e) box and whisker plot of Pineo Ridge moraine complex ^{10}Be ages.

Tables

Table 1: ^{10}Be ages from Acadia National Park and the Pineo Ridge moraine complex.

Sample	Location	Lat (DD) ^a	Lon (DD)	Elev (m asl)	Sample type	Thickness (cm)	^{10}Be conc (10^4 atoms g^{-1}) ^b	^{10}Be unc (1σ) (10^4 atoms g^{-1})	Age (ka) ^c	Internal uncertainty (1σ) (ka)	External uncertainty (1σ) (ka)
MDI-03	Pemetic Mt.	44.33703	68.24551	374	boulder	2	8.12	0.16	14.9	0.3	0.8
MDI-04	Pemetic Mt.	44.33703	68.24552	374	bedrock	2	8.03	0.26	14.7	0.5	0.9
MDI-05	Pemetic Mt.	44.33477	68.24505	374	boulder	1	8.59	0.18	15.5	0.3	0.8
MDI-06	Pemetic Mt.	44.33477	68.24505	374	bedrock	5	7.76	0.19	14.6	0.4	0.8
MDI-07	Pemetic Mt.	44.33211	68.24359	351	boulder	1.5	8.39	0.16	15.8	0.3	0.8
MDI-08	Pemetic Mt.	44.33211	68.24359	351	bedrock	1.5	7.86	0.15	14.7	0.3	0.8
MDI-09	Pemetic Mt.	44.32898	68.24300	285	boulder	1.5	7.82	0.15	15.5	0.3	0.8
MDI-10	Pemetic Mt.	44.32898	68.24300	285	bedrock	4	7.43	0.15	15.0	0.3	0.8
MDI-11	Pemetic Mt.	44.32645	68.24426	245	boulder	1.5	7.27	0.14	15.2	0.3	0.8
MDI-12	Pemetic Mt.	44.32645	68.24426	245	bedrock	3	7.21	0.24	15.1	0.5	0.9
MDI-13	Pemetic Mt.	44.32366	68.24363	178	boulder	3	6.84	0.14	15.7	0.3	0.8
MDI-14	Pemetic Mt.	44.32372	68.24401	170	bedrock	1.5	6.51	0.16	14.5	0.4	0.8
MDI-15	Jordan Pond	44.32426	68.25177	86	boulder	1.5	5.76	0.11	13.9	0.3	0.7
MDI-16	Jordan Pond	44.32426	68.25177	86	boulder	2	5.08	0.11	12.1	0.3	0.6
MDI-17	Jordan Pond	44.32389	68.25298	81	boulder	4	5.86	0.13	14.3	0.3	0.8
MDI-18	Jordan Pond	44.32390	68.25244	87	boulder	1	5.42	0.12	13.0	0.3	0.7
MDI-19	Jordan Pond	44.32391	68.25242	86	boulder	1.5	3.74	0.10	8.9	0.2	0.5
MDI-20	Jordan Pond	44.32388	68.25264	85	boulder	1.5	5.59	0.14	13.3	0.3	0.7
MDI-21	Cadillac Mt.	44.35244	68.22646	460	boulder	2	8.83	0.19	15.0	0.3	0.8
MDI-22	Cadillac Mt.	44.35244	68.22646	460	bedrock	2	9.50	0.27	16.2	0.5	0.9
MDI-23	Sargent Mt.	44.34106	68.27230	404	boulder	2.5	6.31	0.13	11.3	0.2	0.6
MDI-24	Sargent Mt.	44.34106	68.27230	404	bedrock	2.5	8.51	0.22	15.3	0.4	0.8
MDI-25	Penobscot Mt.	44.32363	68.26296	217	boulder	2	5.86	0.12	12.4	0.2	0.6
MDI-26	Penobscot Mt.	44.32236	68.26296	217	bedrock	5	7.04	0.14	15.3	0.3	0.8
PR-14-1	Pineo Ridge	44.67295	67.82355	74	boulder	1.5	6.43	0.19	15.3	0.4	0.9
PR-14-2	Pineo Ridge	44.67295	67.82355	74	boulder	4.0	5.90	0.12	14.3	0.3	0.7

PR-14-3	Pineo Ridge	44.67305	67.82213	72	boulder	1.0	5.94	0.12	14.1	0.3	0.7
PR-14-4	Pineo Ridge	44.67253	67.81900	62	boulder	1.0	6.21	0.12	14.9	0.3	0.8
PR-14-5	Pineo Ridge	44.67253	67.81900	62	boulder	1.0	6.08	0.18	14.6	0.4	0.8
PR-14-6	Pineo Ridge	44.67255	67.82676	77	boulder	2.5	5.97	0.16	14.3	0.4	0.8
PR-14-7	Pineo Ridge	44.67293	67.82713	77	boulder	1.5	5.85	0.17	13.9	0.4	0.8

^aDD = Decimal Degrees

^bBe measurements were normalized to standard 07KNSTD3110 (assumed ratio of 2.850×10^{-15}) and corrected for blanks ($6.22 \pm 4.91 \times 10^{-16}$, n=3)

^cExposure ages were calculated with the CRONUS-Earth online calculator v.2.2 and constants v.2.1 (Balco et al., 2008) using the northeastern North American production rate (Balco et al., 2009) and the Lal (1991)/Stone (2000) constant production rate and scaling scheme, assuming no erosion, no inheritance, and a density of 2.7 g cm^{-3}

Supplementary Material

Inferred ^{14}C Reservoir Effect

We infer a 1,200 ^{14}C year deglacial marine reservoir effect based on the mean of the Acadia National Park dipstick ^{10}Be ages (15.2 ± 0.7 ka) in comparison to the 16.1 ka (13.4 ^{14}C ka) isochron drawn through coastal Maine by Borns et al. (2004), who used a 600 year reservoir correction. Because this reservoir correction is apparently too small, we tried subtracting reservoir corrections of 800, 1000, 1200 years from the raw ^{14}C age of the Borns et al. isochron (14 ^{14}C ka). We then calibrated each corrected ^{14}C age using CALIB 7.1:

Marine Res Correction (yr)	Corrected ^{14}C age (^{14}C ka)	Calibrated Age (ka; 2σ)
600	13.4	15.9 – 16.3
800	13.2	15.6 – 16.1
1000	13.0	15.3 – 15.8
1200	12.8	15.0 – 15.5

The 1,200 year reservoir correction yields the best agreement with our mean Acadia ^{10}Be age, and thus we favor this.

We also base the 1,200 ^{14}C year reservoir correction on the maximum and minimum radiocarbon estimates for the PRMC (13.4 and 12.8 ^{14}C ka) from Kaplan (2007). The original author used a 400 and 600 year correction (i.e., 13.8 and 13.4 ^{14}C ka uncorrected). We found that a 1,200 ^{14}C reservoir correction yields radiocarbon ages that best overlap with our PRMC mean ^{10}Be age of 14.5 ± 0.7 ka.

Marine Res Correction (yr)	Corrected ^{14}C Age (^{14}C ka)	Calibrated Age (ka, 2σ)
400	13.4 – 13.0	16.1 – 15.5
600	13.2 – 12.8	15.8 – 15.2
800	13.0 – 12.6	15.5 – 15.0
1000	12.8 – 12.4	15.2 – 14.5
1200	12.6 – 12.2	15.0 – 14.0

Isostatic Uplift Correction

We recalculated ^{10}Be ages taking into account isostatic uplift using the time-averaged elevation of our sample sites computed with the uplift history (at 44.5°N, 68.5°W) from the ICE-6G model (Peltier et al., 2015). This correction increases exposure ages by ~1%.

Time (ka)	Uplift (m)	Sample Name	Current Elevation (m)	Time-averaged Elevation Since Deglaciation (m)	Age (ka)	Uplift-corrected Age (ka)
15.5	118.5	MDI-03	374	363	14.9	15.1
15	106.1	MDI-04	374	363	14.7	14.9
14.5	98.2	MDI-05	374	363	15.5	15.7
14	74.9	MDI-06	374	363	14.6	14.8
13.5	54.7	MDI-07	351	340	15.8	16.0
13	39.2	MDI-08	351	340	14.7	14.8
12.5	25.1	MDI-09	285	274	15.5	15.7
12	13.7	MDI-10	285	274	15.0	15.2
11.5	2.4	MDI-11	245	234	15.2	15.4
11	-0.5	MDI-12	245	234	15.1	15.3
10.5	-6.4	MDI-13	178	167	15.7	15.9
10	-10.8	MDI-14	170	159	14.5	14.6
9.5	-13.7	MDI-15	86	75	13.9	14.1
9	-15.1	MDI-16	86	75	12.2	12.3
8.5	-16	MDI-17	81	70	14.3	14.5
8	-16.1	MDI-18	87	76	13.0	13.2
7.5	-15.6	MDI-19	86	75	8.9	9.0
7	-14.2	MDI-20	85	74	13.4	13.5
6.5	-12	MDI-21	460	449	15.0	15.2
6	-10.7	MDI-22	460	449	16.2	16.4
5.5	-9.2	MDI-23	404	393	11.3	11.4
5	-7.8	MDI-24	404	393	15.3	15.5

4.5	-6.5
4	-5.2
3.5	-4.3
3	-3.4
2.5	-2.7
2	-2
1.5	-1.4
1	-1
0.5	-0.4
0	0
Average	11.2

MDI-25	217	206	12.4	12.5
MDI-26	217	206	15.3	15.4
PR-14-1	74	63	15.3	15.5
PR-14-2	74	63	14.3	14.5
PR-14-3	72	61	14.1	14.3
PR-14-4	62	51	14.9	15.1
PR-14-5	62	51	14.6	14.8
PR-14-6	77	66	14.3	14.5
PR-14-7	77	66	13.9	14.0

Supplementary Tables

Supplemental Table S1: Published radiocarbon data used in Fig. 1

Lab Code	Latitude (N°)	Longitude (W°)	Material	¹⁴ C Age (yr BP)	Calibrated median age (yr BP)	Calibrated 2σ age range (yr BP)	Calibration ^{1,2}	Reference
AA-10162	43.9640	69.9820	<i>Portlandia arctica</i>	13315 ± 90	15432	15157 - 15734	MARINE13	Retelle & Weddle, 2001; Borns et al., 2004
AA-10165	44.0640	70.1930	<i>Portlandia arctica</i>	12890 ± 85	14671	14231 - 15084	MARINE13	Retelle & Weddle, 2001; Borns et al., 2004
AA-10166	43.6060	70.4300	<i>Portlandia arctica</i>	14820 ± 105	17570	17254 - 17881	MARINE13	Retelle & Weddle, 2001, Borns et al., 2004
AA-7461	44.6686	67.2500	<i>Nucula tenuis</i>	13810 ± 90	16129	15832 - 16402	MARINE13	Kaplan, 1999; Dorion et al., 2001
AA-7462	44.6642	67.3186	<i>Portlandia arctica</i>	13370 ± 90	15503	15214 - 15801	MARINE13	Kaplan, 1999; Dorion et al., 2001
AA-7463	44.9930	69.3190	<i>Portlandia arctica</i>	13290 ± 85	15394	15137 - 15696	MARINE13	Dorion et al., 2001; Borns et al., 2004
AA-8213	44.8131	66.9794	<i>Hiatella arctica</i>	13150 ± 150	15159	14465 - 15710	MARINE13	Kaplan, 1999; Dorion et al., 2001

AA-9107	43.2368	70.1170	forams	14760 ± 215	17468	16860 - 18004	MARINE13	Schnitker et al., 2001
AA-9110	42.4757	68.4613	forams	15480 ± 115	18317	18007 - 18597	MARINE13	Schnitker et al., 2001
AA-9293	45.1700	68.9240	<i>Portlandia arctica</i>	13075 ± 90	15055	14609 - 15365	MARINE13	Dorion et al., 2001; Borns et al., 2004
DIC-1596	44.2114	69.2747	shells	12220 ± 115	13675	13416 - 13942	MARINE13	Smith, 1985
DIC-1600	44.1203	69.2406	shells	12160 ± 105	13614	13382 - 13856	MARINE13	Smith, 1985
GX-20774	43.9000	69.9500	<i>Hiatella arctica</i>	13100 ± 125	15074	14452 - 15563	MARINE13	Retelle & Weddle, 2001
GX-21623	43.9500	69.9500	<i>Mesodesma arctatum</i>	13240 ± 190	15306	14507 - 15941	MARINE13	Retelle & Weddle, 2001
GX-21939	43.8210	69.8400	<i>Mytilus edulis</i>	13600 ± 380	15803	14472 - 16984	MARINE13	Retelle & Weddle, 2001
GX-28135	43.9500	69.9500	<i>Balanus sp.</i>	12780 ± 90	14453	14086 - 14929	MARINE13	Weddle, 2001 (MGS web site)
OS-11022	45.2040	69.1810	<i>Macoma balthica</i>	13550 ± 60	15790	15554 - 16030	MARINE13	Dorion et al., 2001; Borns et al., 2004
OS-1314	44.6686	67.2500	<i>Macoma calcarea</i>	13650 ± 55	15922	15725 - 16116	MARINE13	Kaplan, 1999
OS-1322	45.5873	68.4568	<i>Portlandia arctica</i>	13450 ± 75	15622	15315 - 15886	MARINE13	Dorion et al., 2001; Borns et al., 2004
OS-1842	42.4695	67.1103	forams	14850 ± 60	17607	17415 - 17851	MARINE13	Schnitker et al., 2001
OS-1852	42.4390	67.1305	forams	12900 ± 45	14724	14325 - 15046	MARINE13	Schnitker et al., 2001
OS-1853	43.1288	68.3847	forams	16750 ± 85	19734	19512 - 19988	MARINE13	Schnitker et al., 2001
OS-1859	42.9377	67.3583	forams	15050 ± 45	17832	17660 - 17993	MARINE13	Schnitker et al., 2001
OS-1863	43.3567	69.4557	forams	15200 ± 50	17996	17831 - 18172	MARINE13	Schnitker et al., 2001
OS-18899	43.9030	70.0990	<i>Portlandia arctica</i>	13000 ± 55	14951	14653 - 15196	MARINE13	Retelle & Weddle, 2001; Born et al., 2004
OS-2075	44.8131	66.9794	<i>Nucula tenuis</i>	13800 ± 80	16117	15843 - 16353	MARINE13	Kaplan, 1999; Dorion et al., 2001
OS-2151	44.8283	67.1017	<i>Hiatella arctica</i>	13350 ± 50	15470	15264 - 15698	MARINE13	Kaplan, 1999; Dorion et al., 2001
OS-2152	44.7203	67.3100	<i>Nucula expansa</i>	12900 ± 50	14720	14313 - 15051	MARINE13	Kaplan, 1999
OS-2154	44.6417	67.2417	<i>Macoma calcarea</i>	14000 ± 85	16386	16108 - 16696	MARINE13	Kaplan, 1999; Dorion et al., 2001
OS-2155	44.7500	67.4203	<i>Hiatella arctica</i>	12800 ± 50	14458	14149 - 14800	MARINE13	Kaplan, 1999; Dorion et al., 2001

OS-2659	45.0337	67.1080	<i>Nucula tenuis</i>	12900 ± 50	14720	14313 - 15051	MARINE13	Dorion et al., 2001
OS-2660	44.8237	66.1010	<i>Mytilus edulis</i>	13000 ± 65	14940	14551 - 15210	MARINE13	Dorion et al., 2001
OS-2661	45.1250	67.5390	<i>Portlandia arctica</i>	13200 ± 60	15246	15065 - 15510	MARINE13	Dorion et al., 2001; Borns et al., 2004
OS-2662	44.5430	69.0570	forams	13000 ± 60	14946	14602 - 15208	MARINE13	Dorion et al., 2001; Borns et al., 2004
OS-2663	45.1368	67.1242	<i>Nucula tenuis</i>	13700 ± 70	15988	15758 - 16213	MARINE13	Dorion et al., 2001
OS-3160	45.3673	68.5425	<i>Nucula tenuis</i>	13300 ± 65	15402	15176 - 15661	MARINE13	Dorion et al., 2001; Borns et al., 2004
OS-3161	44.7580	67.5050	<i>Nucula tenuis</i>	13300 ± 65	15402	15176 - 15661	MARINE13	Dorion et al., 2001
OS-3465	44.8780	67.3850	seaweed	13400 ± 95	15544	15236 - 15858	MARINE13	Dorion et al., 2001; Borns et al., 2004
OS-3466	44.5950	68.0230	<i>Nucula tenuis</i>	12950 ± 120	14780	14223 - 15204	MARINE13	Dorion et al., 2001
OS-4419	43.8500	70.2000	<i>Mytilus edulis</i>	13300 ± 50	15396	15198 - 15623	MARINE13	Retelle & Weddle, 2001
OS-7135	44.8131	66.9794	<i>Hiatella arctica</i>	13350 ± 50	15470	15264 - 15698	MARINE13	Dorion et al., 2001
Pitt-743	43.5250	70.3167	<i>Macoma balthica</i>	14490 ± 450	17062	15841 - 18215	MARINE13	Kelley et al., 1992
QL-192	43.3839	70.5453	<i>Mytilus edulis</i>	13830 ± 100	16154	15842 - 16474	MARINE13	Smith, 1985; Retelle & Weddle, 2001
RIDDL-814	42.4400	69.8637	forams	17660 ± 130	20814	20477 - 21203	MARINE13	Schnitker et al., 2001
SI-1048	44.5000	67.1167	shells	12575 ± 120	14087	13770 - 14633	MARINE13	Dyke, 2004
SI-2712a	43.7664	69.3119	shells	12680 ± 100	14259	13923 - 14763	MARINE13	Belknap et al., 1987
SI-4649	44.3050	69.9775	shells	12845 ± 100	14577	14154 - 15049	MARINE13	Smith, 1985
SI-4651	44.1583	68.4300	shells	13305 ± 110	15422	15106 - 15775	MARINE13	Smith, 1985
SI-4745b	43.7964	70.2594	shells	12745 ± 100	14397	14022 - 14905	MARINE13	Smith, 1985
SI-5371	44.9833	69.3167	<i>Portlandia arctica</i>	13280 ± 410	15291	13971 - 16479	MARINE13	Anderson et al., 1992
SI-7017	43.9500	69.9500	<i>Mytilus edulis</i>	13220 ± 120	15291	14866 - 15729	MARINE13	Retelle & Bither, 1989
W-1011	44.8167	68.9667	<i>Astarte crenata suba</i>	13200 ± 450	15160	13807 - 16468	MARINE13	Dyke, 2004
W-2117	43.8639	69.6444	<i>Mytilus edulis</i>	12780 ± 350	14548	13560 - 15619	MARINE13	Dyke, 2004
Y-1477	44.9100	69.9389	<i>Macoma balthica</i>	13420 ± 240	15565	14737 - 16289	MARINE13	Stuiver & Borns, 1975

Y-2200	44.7069	67.3156	<i>Nucula expansa</i>	12930 ± 160	14726	14127 - 15257	MARINE13	Stuiver & Borns, 1975
Y-2201a	44.6619	67.3128	<i>Mytilus edulis</i>	12420 ± 120	13899	13586 - 14176	MARINE13	Stuiver & Borns, 1975
Y-2201b	44.6619	67.3128	seaweed	12480 ± 250	14043	13426 - 14953	MARINE13	Stuiver & Borns, 1975
Y-2208	43.3736	70.5250	<i>Hiatella arctica</i>	13600 ± 120	15847	15420 - 16202	MARINE13	Stuiver & Borns, 1975
Y-2212	43.9719	70.0278	<i>Macoma calcarea, Mya</i>	12960 ± 160	14777	14143 - 15297	MARINE13	Stuiver & Borns, 1975
Y-2214	44.3128	68.8292	Balanus sp.	13180 ± 160	15211	14494 - 15773	MARINE13	Stuiver & Borns, 1975
Y-2217	44.6686	67.2500	seaweed	13720 ± 200	16001	15347 - 16571	MARINE13	Stuiver & Borns, 1975
OS-61188	43.6500	70.2800	<i>Mytilus edulis</i> valve	12850 ± 65	14576	14202 - 14984	MARINE13	Thompson et al., 2011
OS-60406	43.6500	70.2800	Barnacle fragments	12800 ± 55	14462	14143 - 14822	MARINE13	Thompson et al., 2011
OS-60388	43.6500	70.2800	<i>Macoma balthica</i> valve	12650 ± 55	14150	13954 - 14430	MARINE13	Thompson et al., 2011
OS-60390	43.6500	70.2800	<i>Serripes groenlandicus</i> valve	12500 ± 55	13983	13825 - 14132	MARINE13	Thompson et al., 2011
OS-60389	43.6500	70.2800	unidentified valve fragments	12350 ± 90	13823	13580 - 14052	MARINE13	Thompson et al., 2011
AA-1935	46.4110	69.0490	wood fragments	10480 ± 130	12365	11986 - 12697	IntCal13	Davis, RB in Borns et al., 2004
AA-9506	44.8333	70.5833	terrestrial vegetation	11665 ± 85	13496	13314 - 13645	IntCal13	Thompson et al., 1999; Borns et al., 2004
AA-9508	44.9310	70.5420	terrestrial vegetation	10490 ± 75	12428	12115 - 12635	IntCal13	Borns et al., 2004
Beta-10110	45.2333	69.9833	charcoal	10110 ± 70	11712	11392 - 12020	IntCal13	Martindale et al., 2016
Beta-101669	45.0417	68.7333	gyttja	9540 ± 80	10890	10652 - 11161	IntCal13	Almquist et al., 2001
Beta-126645	44.1000	70.4500	charcoal	10240 ± 90	11970	11612 - 12395	IntCal13	Martindale et al., 2016
Beta-1833	45.2500	70.0000	charcoal	11120 ± 180	12979	12702 - 13300	IntCal13	Gramley & Rutledge, 1981
Beta-24945	43.9230	69.1430	cedar(?) twig	11770 ± 160	13609	13287 - 13988	IntCal13	Kellogg, 1989; Borns et al., 2004
Beta-43725	44.8510	68.0290	<i>Picea</i> needles	11620 ± 100	13448	13262 - 13642	IntCal13	Doner, 1995; Borns et al., 2004

Beta-65420	46.2890	67.8750	woody twig	11560 ± 60	13392	13270 - 13494	IntCal13	Doner, 1995; Borns et al., 2004
Beta-70668	43.5000	70.5000	charcoal	10580 ± 60	12564	12412 - 12688	IntCal13	Martindale et al., 2016; Speiss & Mosher, 1994
Beta-7183	45.2350	68.9631	charcoal	10290 ± 460	11937	10691 - 13047	IntCal13	Martindale et al., 2016; Speiss, 1995
Beta-90768	46.4360	68.3880	peat	10530 ± 90	12470	12136 - 12684	IntCal13	Borns et al., 2004
GSC-1248	45.5667	70.6750	gyttja	11200 ± 160	13053	12731 - 13334	IntCal13	Mott, 1977
GX-22125	45.6667	70.1667	gyttja	10475 ± 275	12244	11324 - 12819	IntCal13	Balco et al., 1998
GX-22922	43.7500	69.8000	lake sed	13230 ± 220	15877	15223 - 16507	IntCal13	Retelle & Weddle, 2001
Hel-1716	44.2333	68.3167	basal peat	10980 ± 190	12882	12564 - 13228	IntCal13	Tolonen & Tolonen, 1984
I-5118	44.5833	69.9167	lake sed	11330 ± 200	13183	12780 - 13546	IntCal13	Davis & Jacobsen, 1985
I-5639	44.6275	68.6392	gyttja	13510 ± 300	16289	15362 - 17150	IntCal13	Davis et al., 1975; Borns et al., 2004
Not given	45.3333	70.7500	lake sed	10860 ± 160	12780	12523 - 13084	IntCal13	Borns & Calkin, 1977
not given 22 (Y)	45.0800	71.0800	basal peat	10860 ± 160	12780	12523 - 13084	IntCal13	Borns & Calkin, 1977
not given 23 (Y)	45.0800	71.0800	basal peat	10480 ± 160	12339	11922 - 12713	IntCal13	Borns & Calkin, 1977
OS-12839	43.4630	70.8070	lake sed	13350 ± 75	16061	15810 - 16280	IntCal13	Thompson, 2001 citing Dorion; Borns et al., 2004
OS-14150	46.4230	69.6680	<i>Salix herbacea</i>	11150 ± 85	13005	12789 - 13166	IntCal13	Dorion, 1998; Borns et al., 2004
OS-15398	44.8500	68.0280	insect & plant parts	12850 ± 65	15329	15127 - 15596	IntCal13	Lurvey, 1999; Borns et al., 2004
OS-2093	44.8530	68.0940	terrestrial vegetation	12350 ± 55	14363	14105 - 14718	IntCal13	Borns et al., 2001
OS-2682	45.2420	68.3940	terrestrial vegetation	10450 ± 50	12364	12122 - 12546	IntCal13	Borns et al., 2001
OS-3002	46.6150	68.0050	terrestrial vegetation	11950 ± 190	13816	13340 - 14361	IntCal13	Borns et al., 2001
OS-4383	47.2130	68.4680	terrestrial vegetation	10600 ± 30	12598	12531 - 12682	IntCal13	Borns et al., 2001
OS-4416	43.8000	70.4500	<i>Populus balsamifera</i>	12100 ± 110	13961	13707 - 14303	IntCal13	Thompson, 2001; Borns et al., 2004

OS-4839	46.7110	67.8110	lake sed	12750 ± 40	15193	15047 - 15335	IntCal13	Borns et al., 2004
OS-4842	45.3430	68.0520	insect parts	11000 ± 40	12857	12737 - 12991	IntCal13	Borns et al., 2004
OS-4843	45.0160	68.0630	terrestrial vegetation	12200 ± 60	14092	13855 - 14290	IntCal13	Borns et al., 2004
OS-4844	45.4780	68.0640	terrestrial vegetation	11700 ± 50	13519	13422 - 13615	IntCal13	Borns et al., 2004
OS-5303	47.0610	68.9060	terrestrial vegetation	11500 ± 60	13348	13219 - 13462	IntCal13	Borns et al., 2004
OS-5305	46.5140	67.9500	terrestrial vegetation	12800 ± 100	15265	14920 - 15653	IntCal13	Borns et al., 2004
OS-5992	45.6540	68.3010	insect parts	10300 ± 55	12098	11933 - 12252	IntCal13	Borns et al., 2004
OS-5993	46.8110	68.0660	terrestrial vegetation	11000 ± 160	12892	12654 - 13169	IntCal13	Borns et al., 2004
OS-6148	46.3980	68.3480	terrestrial vegetation	11200 ± 75	13066	12843 - 13218	IntCal13	Borns et al., 2004
OS-6440	45.5770	69.0390	terrestrial vegetation	11650 ± 100	13480	13292 - 13715	IntCal13	Borns et al., 2004
OS-6582	45.7960	68.1600	terrestrial vegetation	11000 ± 60	12867	12728 - 13016	IntCal13	Borns et al., 2004
OS-6683	47.0710	68.6560	moss	10900 ± 90	12792	12682 - 13000	IntCal13	Borns et al., 2004
OS-6794	45.6667	70.1667	needles	8370 ± 40	9405	9293 - 9479	IntCal13	Balco et al., 1998
OS-7119	44.6750	70.8650	<i>Salix herbacea</i>	12250 ± 55	14158	13979 - 14450	IntCal13	Thompson et al., 1999
OS-7122	44.2200	70.8320	insect parts	13150 ± 50	15799	15599 - 16012	IntCal13	Thompson et al., 1999
OS-7123	45.2600	70.9570	insect parts	11500 ± 50	13349	13252 - 13456	IntCal13	Thompson et al., 1999
OS-8339	45.6667	70.1667	plants	10050 ± 45	11563	11328 - 11772	IntCal13	Balco et al., 1998
SI-2992	45.8250	68.8810	lake sed	11630 ± 260	13479	12973 - 14097	IntCal13	Davis & Davis, 1980; Borns et al., 2004
SI-3702	47.2300	68.0100	basal peat	9720 ± 70	11134	11062 - 11251	IntCal13	Rampton et al., 1984
SI-3783	46.0833	68.9000	lake sed	9970 ± 110	11488	11202 - 11831	IntCal13	Anderson et al., 1986
SI-4042	44.3360	68.2690	lake sed	13230 ± 360	15861	14671 - 17021	IntCal13	Smith, 1985; Borns et al., 2004
SI-4043	44.2500	68.2500	lake sed	11355 ± 125	13210	12992 - 13459	IntCal13	Smith, 1985; Lowell, 1989
SI-4462	46.0833	68.9000	lake sed	10925 ± 220	12836	12388 - 13283	IntCal13	Anderson et al., 1986

SI-4463	46.0833	68.9000	plant macrofossils	10965 ± 230	12869	12403 - 13314	IntCal13	Anderson et al., 1986; Borns et al., 2004
SI-4656	44.0333	70.3500	plant macrofossils	12860 ± 325	15286	14133 - 16223	IntCal13	Davis & Jacobsen, 1985; Borns et al., 2004
SI-4657	43.9610	70.3420	plant macrofossils	12710 ± 125	15105	14497 - 15592	IntCal13	Davis & Jacobsen, 1985; Borns et al., 2004
SI-4658	47.2960	69.2920	plant macrofossils	10385 ± 140	12230	11750 - 12660	IntCal13	Davis & Jacobsen, 1985; Borns et al., 2004
SI-4933	45.0000	68.8600	basal peat	9450 ± 100	10723	10480 - 11109	IntCal13	Tolonen et al., 1988
SI-4953	45.0390	68.2000	plant macrofossils	12615 ± 115	14920	14309 - 15297	IntCal13	Davis & Jacobsen, 1985; Borns et al., 2004
SI-5135	44.7330	66.9670	basal peat	10385 ± 95	12251	11948 - 12561	IntCal13	Tolonen & Tolonen, 1984
SI-5905	44.2500	68.2500	peat	10085 ± 125	11664	11246 - 12086	IntCal13	Dyke, 2004
TO-4403	45.0833	68.1833	wood	10840 ± 90	12744	12612 - 12967	IntCal13	Cwynar & Levesque, 1995
Y-1249	45.2200	68.7200	basal peat	10040 ± 120	11590	11239 - 12009	IntCal13	Stuiver et al., 1963
Y-1251	45.2200	68.5800	basal peat	9620 ± 150	10944	10515 - 11290	IntCal13	Stuiver et al., 1963
Y-1252	45.5000	68.5500	basal peat	9960 ± 150	11504	11103 - 12051	IntCal13	Stuiver et al., 1963
Y-1253	45.8200	68.4300	basal peat	10140 ± 120	11763	11267 - 12165	IntCal13	Stuiver et al., 1963
Y-1254	44.8000	68.9000	basal peat	9610 ± 120	10942	10651 - 11231	IntCal13	Stuiver et al., 1963
Y-1255	45.0700	69.9000	basal peat	9410 ± 120	10664	10366 - 11091	IntCal13	Stuiver et al., 1963
Y-1256	45.4500	67.7500	basal peat	10560 ± 150	12454	12019 - 12731	IntCal13	Stuiver et al., 1963
Y-1257	45.4300	67.6800	basal peat	9120 ± 160	10296	9765 - 10702	IntCal13	Stuiver et al., 1963
Y-1258	44.9300	68.7000	basal peat	9730 ± 160	11097	10646 - 11622	IntCal13	Stuiver et al., 1963
Y-1259	46.2200	67.8700	base of bog	9440 ± 150	10722	10369 - 11166	IntCal13	Stuiver et al., 1963
Y-1260	44.4800	69.9500	basal peat	9630 ± 150	10952	10544 - 11316	IntCal13	Stuiver et al., 1963
Y-1460	44.4300	69.2250	basal peat in kettle	11750 ± 160	13587	13273 - 13973	IntCal13	Stuiver & Borns, 1975
Y-1479	44.6306	69.0103	peat in kettle	12220 ± 240	14261	13585 - 15083	IntCal13	Stuiver & Borns, 1975
Y-1479	44.6300	69.0100	basal peat in kettle	12220 ± 240	14261	13585 - 15083	IntCal13	Stuiver & Borns, 1975
Y-1967	44.6700	67.9200	basal peat	9710 ± 160	11060	10584 - 11504	IntCal13	Radiocarbon 5
Y-2218	44.6900	67.8700	wood base of peat	10060 ± 120	11621	11244 - 12032	IntCal13	Stuiver & Borns, 1975

Y-2219	44.7200	67.9100	silt at base of peat	10530 ± 160	12410	11953 - 12731	IntCal13	Stuiver & Borns, 1975
Y-2220	44.8280	68.0800	basal organic sediment	13760 ± 100	16632	16300 - 16977	IntCal13	Stuiver & Borns, 1975
Y-2221	44.9200	68.1000	silt at base of peat	11840 ± 100	13660	13453 - 13861	IntCal13	Stuiver & Borns, 1975
Y-2464	45.0800	71.0800	basal peat in kettle	10030 ± 180	11612	11140 - 12240	IntCal13	Borns & Calkin, 1977
Beta-240351	44.3340	68.2700	organic sediment	13260 ± 50	15942	15747 - 16125	IntCal13	Norton et al., 2011

¹All radiocarbon ages were calibrated with CALIB 7.1

²All marine samples were calibrated with MARINE13, which uses a 405 year marine reservoir correction

Supplementary Table S2: Acadia National Park and Pineo Ridge moraine complex ¹⁰Be data

Cathode Number	Sample Name	Shielding	Measured ¹ ¹⁰ Be/ ⁹ Be	Measured ¹⁰ Be/ ⁹ Be Uncertainty (1σ)	Blank-corrected ² ¹⁰ Be/ ⁹ Be	Blank-corrected ² ¹⁰ Be/ ⁹ Be Uncertainty (1σ)	Quartz Mass (g)	Mass of Added ⁹ Be (μg)
BE40756	MDI-03	0.99	1.20E-13	2.24E-15	1.20E-13	2.29E-15	22.1653	224.8
BE40757	MDI-04	0.99	1.19E-13	3.85E-15	1.18E-13	3.88E-15	22.3911	227.3
BE40759	MDI-05	1	1.31E-13	2.64E-15	1.31E-13	2.69E-15	10.1624	227.0
BE40760	MDI-06	0.99	1.12E-13	2.68E-15	1.11E-13	2.72E-15	23.0691	224.6
BE40761	MDI-07	0.98	1.27E-13	2.38E-15	1.26E-13	2.43E-15	21.5504	225.5
BE40762	MDI-08	0.99	1.18E-13	2.22E-15	1.17E-13	2.28E-15	22.6986	224.9
BE40764	MDI-09	0.99	1.19E-13	2.23E-15	1.18E-13	2.28E-15	22.3482	226.4
BE40765	MDI-10	0.99	1.13E-13	2.26E-15	1.12E-13	2.32E-15	22.8501	222.1
BE40766	MDI-11	0.97	1.13E-13	2.11E-15	1.12E-13	2.16E-15	22.4001	224.1
BE40767	MDI-12	0.98	9.96E-14	3.21E-15	9.90E-14	3.24E-15	23.0707	243.8
BE40768	MDI-13	0.95	1.08E-13	2.07E-15	1.08E-13	2.13E-15	22.3598	224.8
BE40769	MDI-14	0.98	9.51E-14	2.29E-15	9.45E-14	2.34E-15	23.6195	228.2
BE40770	MDI-15	0.98	8.66E-14	1.57E-15	8.60E-14	1.65E-15	22.1437	225.5
BE40772	MDI-16	0.99	7.69E-14	1.56E-15	7.63E-14	1.64E-15	22.4755	225.5
BE40773	MDI-17	0.99	8.68E-14	1.90E-15	8.61E-14	1.96E-15	10.5686	225.6

BE40774	MDI-18	0.98	8.16E-14	1.71E-15	8.10E-14	1.78E-15	22.6464	225.4
BE40775	MDI-19	0.99	5.63E-14	1.46E-15	5.57E-14	1.54E-15	22.1547	225.7
BE40777	MDI-20	0.99	8.36E-14	2.08E-15	8.29E-14	2.13E-15	22.5065	224.7
BE40778	MDI-21	0.99	1.36E-13	2.80E-15	1.36E-13	2.84E-15	22.4793	225.1
BE40779	MDI-22	0.99	1.43E-13	3.99E-15	1.43E-13	4.02E-15	22.2716	223.5
BE40792	MDI-23	0.99	9.69E-14	1.93E-15	9.63E-14	1.99E-15	23.1088	225.2
BE40793	MDI-24	0.99	1.29E-13	3.32E-15	1.28E-13	3.36E-15	22.4065	226.2
BE40794	MDI-25	0.99	8.76E-14	1.66E-15	8.70E-14	1.73E-15	22.9775	225.2
BE40795	MDI-26	0.99	9.55E-14	1.80E-15	9.48E-14	1.87E-15	22.8059	226.1
BE40796	PR-14-1	1	1.00E-13	2.85E-15	9.95E-14	2.89E-15	22.3343	225.3
BE40797	PR-14-2	1	8.86E-14	1.66E-15	8.79E-14	1.73E-15	20.3636	224.5
BE40798	PR-14-3	1	8.25E-14	1.64E-15	8.19E-14	1.71E-15	23.2922	224.7
BE40799	PR-14-4	1	9.75E-14	1.81E-15	9.69E-14	1.87E-15	22.3752	225.8
BE40800	PR-14-5	1	9.06E-14	2.67E-15	9.00E-14	2.72E-15	20.6927	226.2
BE40801	PR-14-6	1	9.54E-14	2.48E-15	9.48E-14	2.53E-15	23.5537	225.2
BE40803	PR-14-7	1	8.73E-14	2.45E-15	8.67E-14	2.50E-15	22.3617	224.3

¹Values normalized to standard KNSTD3110 with an assumed ¹⁰Be/⁹Be ratio of 2850 x 10⁻¹⁵ (Nishiizumi et al., 2007)

²Corrected for background using the mean and standard deviation of three full process blanks (6.22 ± 4.91E-16), following the protocol from http://hess.ess.washington.edu/math/docs/common/ams_data_reduction.pdf

Supplementary References

- Almquist, H., Dieffenbacher-Krall, A.C., Flanagan-Brown, R., Sanger, D., 2001. The Holocene record of lake levels of Mansell Pond, central Maine, USA. *The Holocene* 11, 189–201. doi:10.1191/095968301677768783
- Anderson, R.S., Davis, R.B., Miller, N.G., Stuckenrath, R., 1986. History of the late-and post-glacial vegetation and disturbance around Upper South Branch Pond, northern Maine. *Canadian Journal of Botany* 64, 1977–1986. doi: 10.1139/b86-262
- Anderson, R.S., Jacobson, G.L., Davis, R.B., Stuckenrath, R., 1992. Gould Pond, Maine: late-glacial transitions from marine to upland environments. *Boreas* 21, 359–371
- Balco, G., Belknap, D.F., Kelley, J.T., 1998. Glacioisostasy and Lake-Level Change at Moosehead Lake, Maine. *Quaternary Research* 49, 157–170. doi:10.1006/qres.1998.1962
- Belknap, D.F., Andersen, B.G., Anderson, R.S., Anderson, W.A., Borns Jr., H.W., Jacobson, G.L., Kelley, J.T., Shipp, R.C., Smith, D.C., Stuckenrath, R.J., Thompson, W.B., Tyler, D.A., 1987. Late Quaternary sea-level changes in Maine, in: *Sea-Level Fluctuation and Coastal Evolution*. pp. 71–85.
- Borns Jr., H.W., Calkin, P.E., 1977. Quaternary glaciation, west-central Maine. *Geological Society of America Bulletin* 88, 1773–1784.
- Borns Jr., H.W., Doner, L.A., Dorion, C.C., Jacobson, G.L., Kaplan, M.R., Kreutz, K.J., Lowell, T. V., Thompson, W.B., Weddle, T.K., 2004. The deglaciation of Maine, U.S.A., in: Ehlers, J.E., P.G. (Eds.), *Quaternary Glaciations - Extent and Chronology, Part II*. pp. 89–109.
- Cwynar, L.C., and Levesque, A.J., 1995. Chironomid evidence for late-glacial climatic reversals in Maine, USA. *Quaternary Research* 43, 405–413 doi:10.1006/qres.1995.1046
- Davis, P.T., Davis, R.B., 1980. Interpretation of minimum-limiting radiocarbon dates for deglaciation of Mount Katahdin area, Maine. *Geology* 8, 396–400. doi:10.1130/0091-7613(1980)8<396:IOMRDF>2.0.CO;2
- Davis, R.B., Jacobson, G.L., 1985. Late Glacial and Early Holocene Landsapes in Northern New England and Adjacent Areas of Canada. *Quaternary Research* 23, 341–368.
- Davis, R. B., Bradstreet, J. E., Stuckenrath, R., and Barns, H. W., Jr., 1975. Vegetation and associated environments during the past 14,000 years near Moulton Pond, Maine. *Quaternary Research* 5, 435-466.
- Doner, L.A. 1995. Late-Pleistocene environments in Maine and the Younger Dryas dilemma. M.S. Thesis. University of Maine, Orono, ME. 68 pp.
- Dorion, C.C., Balco, G.A., Kaplan, M.R., Kreutz, K.J., Wright, J.D., Borns, H.W., 2001. Stratigraphy, paleoceanography, chronology, and environment during deglaciation of eastern Maine, in: Weddle, T.K., Retelle, M.J. (Eds.), *Deglacial History and Relative Sea-Level Changes, Northern New England and Adjacent Canada*. pp. 215–242.

- Dorion, C.C., 1998. Style and chronology of deglaciation in central and northern Maine. Geological Society of America, Abstracts with Programs 30, 15.
- Dyke, A.S., 2004. An outline of the deglaciation of North America with emphasis on central and northern Canada. Quaternary Glaciations-Extent and Chronology Part II North America 2b, 373–424. doi:10.1016/S1571-0866(04)80209-4
- Gramly, R. M., & Rutledge, K., 1981. A new Paleo-Indian site in the state of Maine. American Antiquity 46, 354-361.
- Kaplan, M.R., 1999. Retreat of a tidewater margin of the Laurentide ice sheet in eastern coastal Maine between ca. 14 000 and 13 000 14C yr B.P. Geological Society of America Bulletin 111, 620–632. doi:10.1130/0016-7606(1999)111<0620:ROATMO>2.3.CO;2
- Kelley, J.T., Dickson, S.M., Belknap, D.F., and Stuckenrath, R., 1992. Sea-level change and late Quaternary sediment accumulation on the southern Maine inner continental shelf, in Fletcher, C.H., and Wehmiller, J.F., eds., Quaternary coasts of the United States: Marine and lacustrine systems: SEPM Special Publication 40, 23-34.
- Kellogg, D.C., 1988. Problems in the Use of Sea-Level Data for Archaeological Reconstructions. In Holocene Human Ecology in Northeast North America, edited by George P. Nicholas, pp. 81-104. Plenum Press, New York.
- Lowell, T.V., 1989. Late Wisconsin Glacial Geology of the Eastern Portion of Mount Desert Island. In Studies in Maine Geology: Volume 6, edited by R. Tucker and R. Marvinney, pp. 13-32. Maine Geological Survey, Augusta.
- Lurvey, L.K. 1999. An investigation of a glacial landform transition in southeastern Maine. Orono, University of Maine, M.S. Thesis, 79 pp.
- Martindale, A., Morlan, R., Betts, M., Blake, M., Gajewski, K., Chaput, M., Mason, A., and Vermeersch P., 2016. Canadian Archaeological Radiocarbon Database (CARD 2.1).
- Mott, R. J. (1977). Late-Pleistocene and Holocene palynology in southeastern Quebec. Geographie Physique et Quaternaire 31, 139- 149.
- Nishiizumi, K., Imamura, M., Caffee, M.W., Southon, J.R., Finkel, R.C., McAninch, J., 2007. Absolute calibration of ¹⁰Be AMS standards. Nuclear Instruments and Methods in Physics Research Section B: Beam Interactions with Materials and Atoms 258, 403–413. doi:10.1016/j.nimb.2007.01.297
- Norton, S.A., Perry, R.H., Saros, J.E., 2011. The controls on phosphorus availability in a Boreal lake ecosystem since deglaciation. Journal of Paleolimnology 46, 107–122. doi:10.1007/s10933-011-9526-9
- Peltier, W.R., Argus, D.F., Drummond, R., 2015. Space geodesy constrains ice-age terminal deglaciation: The global ICE-6G_C (VM5a) model. J. Geophys. Res. Solid Earth 120, 450-487. doi:10.1002/2014JB011176.
- Rampton, V.N., Gauthier, R.C., Thibault, J. Seaman, A.A., 1984. Quaternary geology of New Brunswick. Geological Survey of Canada, Memoir, 416, 77 pp.

- Retelle, M.J., Weddle, T.K., 2001. Deglaciation and relative sea-level chronology, Casco Bay Lowland and lower Androscoggin River valley, Maine, in: Weddle, T.K., Retelle, M.J. (Eds.), *Deglacial History and Relative Sea-Level Changes, Northern New England and Adjacent Canada*. pp. 191–214.
- Retelle, M. J., and Bither, K. M., 1989. Late Wisconsinan glacial and glaciomarine sedimentary facies in the lower Androscoggin Valley, Topsham, Maine, in Tucker, R.D., and Marvinney, R. G. (Eds), *Studies in Maine geology, Volume 5—Quaternary geology: Augusta, Maine Geological Survey*, 33-52
- Schnitker, D., Belknap, D.F., Bacchus, T.S., Friez, J.K., Lusardi, B.A., Popek, D.M., 2001. Deglaciation of the Gulf of Maine. *Deglacial History and Relative Sea-Level Changes, Northern New England and Adjacent Canada*, 9–34. doi:10.1130/0-8137-2351-5.9
- Smith, G.W., 1985. Chronology of Late Wisconsinan deglaciation of coastal Maine, in: Borns Jr., H.W., LaSalle, P., Thompson, W.B. (Eds.), *Late Pleistocene History of Northeastern New England and Adjacent Quebec*. Geological Society of America, Special Paper 197, 29–44.
- Spiess, A.E., Mosher, J., Callum, K., Sidell, N.A., 1995. Fire on the Plains: Paleo-environmental Data from the Hedden Site. *Maine Archaeological Society Bulletin* 35, 13-52.
- Spiess, A.E. and Mosher, J., 1994. Hedden: A Paleoindian Site on the Kennebunk Plains. *Maine Archaeological Society Bulletin* 34, 25-54.
- Stuiver, M., Deevy, E.S., Rouse, I., 1963. Yale Natural Radiocarbon Measurements VIII. *Radiocarbon* 5, 312-341.
- Stuiver, M., Borns Jr., H.W., 1975. Late quaternary Marine invasion in Maine: Its chronology and associated crustal movement. *Geological Society of America Bulletin* 86, 99–104. doi:10.1130/0016-7606(1975)86<99:LQMIIM>2.0.CO;2
- Thompson, W.B., Fowler, B.K., Dorion, C.C., 1999. Deglaciation of the Northwestern White Mountains, New Hampshire. *Geographie Physique et Quaternaire* 53, 59–77. doi:10.7202/004882ar
- Thompson, W.B., Griggs, C.B., Miller, N.G., Nelson, R.E., Weddle, T.K., Kilian, T.M., 2011. Associated terrestrial and marine fossils in the late-glacial Presumpscot Formation, southern Maine, USA, and the marine reservoir effect on radiocarbon ages. *Quaternary Research* 75, 552–565. doi:10.1016/j.yqres.2011.02.002
- Thompson, W.B., 2001. Deglaciation of western Maine. in Weddle, T.K. and Retelle, M.J. (Eds), *Deglacial history and relative sea-level changes, northern New England and adjacent Canada*. Geological Society of America, Special Paper 351, 109-123.
- Tolonen, K., Tolonen, M., 1984. Late-glacial vegetational succession at four coastal sites in northeastern New England: ecological and phytogeographical aspects *Annales Botanici Fennici* 21, 59–77.
- Tolonen, K., Davis, R. B., & Widoff, L., 1988. Peat accumulation rates in selected Maine peat deposits No. 33. *Maine Geological Survey, Department of Conservation*.